Master Thesis

Wet Gas Compression

Effect of a liquid phase on radial compressor performance

Division of Thermal Power Engineering
Department of Energy Science
Faculty of Engineering

Lund University, Sweden

Author:
Matilda Svensson

Supervisor:
Magnus Genrup

October 31, 2014

Abstract

The aim of the Master Thesis is to analyse the state of the art in wet gas compression, wet gas modelling, derive a thermodynamic model for a compressor layout and compare the model to test data. The Master Thesis is performed at MAN Diesel & Turbo Schweiz AG in Zürich, Switzerland.

Wet gas compression is a discussed topic within the oil and gas business. By reducing the number of components in a gas compression unit, the weight can be reduced and the efficiency of the production can be improved.

A wet gas is defined as a gas with a liquid volume fraction of up to 5 %, which typically corresponds to a mass fraction of up to 70 % depending on the conditions of the mixture, especially suction pressure. Compression of a wet gas contains an evaporation and condensation process and increased losses due to the liquid phase. It is seen that the process cannot be evaluated as a process in thermal equilibrium. Different suction conditions give different results. In general, the required power increases for wet gas compression and the range decreases.

A model for wet gas compression is developed. The model is based on flow models for multi-phase flow in pipes and flow elements. The presented model is based on a dry hydrocarbon gas compressor model with wet gas corrections on the compressor characteristics. It is adapted to MAN inhouse measurement data, which is excluded from this public version of the report.

Popular Scientific Article

Wet Gas Compression -
Effects of a liquid phase on radial compressor performance

Author: Matilda Svensson

Introduction

The research on wet gas compression has a history of more than thirty years. In the beginning, the goal was to understand if compression of a wet gas was possible. Today, the oil and gas industry has a big interest in reducing the size of the compression unit, since many gas fields are located far away from land and in deep water. The pressure in a gas reservoir decreases over time, which means that the gas production declines and in the end ceases [1]. By placing a compression unit directly on the shore bed, as close to the source as possible, the production life can be further extended, since the compression process contributes with benefits like a stable and high gas flow rate and enhancement of the overall recovery [2]. The centrifugal compressor is often used, due to its robustness, high volume flow capacity and traditional usage within the oil and gas industry [3].

In this paper, the performance of compressing wet gas in a radial compressor and a thermodynamic model of compressing wet gas in a radial compresso are presented.

Pressure Ratio

Through a compression process, the pressure is increased. In a centrifugal compression process, radial and axial forces are used to increase the pressure. A common used expression to evaluate the increase in pressure is the *pressure ratio* π

$$\pi = \frac{p_2}{p_1} \tag{1}$$

The pressure ratio expresses the increase in pressure from the suction to the discharge of the compressor or the compressor stage. The efficiency is not handled in this article, since it is not possible to receive trustworthy data of the temperature in the discharge of the compressor.

Basics about Wet Gas

A wet gas is described as a two-phase flow with a liquid and a gas phase. The density for the liquid phase is in general higher than the gas density. The *density ratio* δ is

$$\delta = \frac{\rho_G}{\rho_L} \tag{2}$$

If the density ratio is close to 1, the interaction between the liquid and the gas phase is high, which means that the two-phase flow flows with less losses than for a flow with a low density ratio.

The amount of liquid in a two-phase flow is described with *liquid mass fraction LMF* and *liquid volume fraction LVF*

$$LMF = \frac{\dot{m}_L}{\dot{m}_L + \dot{m}_G} \tag{3a}$$

$$LVF = \frac{\dot{V}_L}{\dot{V}_L + \dot{V}_G} \tag{3b}$$

A wet gas is defined as a two-phase flow with a liquid volume fraction of up to 5 %. The corresponding liquid mass fraction is dependent on the conditions, such as pressure, but can be up to 70 % [4].

Effects of a Wet Gas

Depending on wet gas mixture and suction conditions, the performance of a compressor is different. The liquid phase in a wet gas flow introduces blockage of the compressor. This leads to a decreased maximum flow, earlier choke and a steeper curve, which can be seen in figure 1 and 2. Due to the increased losses and higher flow density for a wet gas flow compared to a dry gas flow, the shaft power increases when compressing a wet gas. For an air/water mixture at 1 bar suction pressure, the pressure ratio is, in general, below the pressure ratio for the dry gas case, see figure 1. For a hydrocarbon mixture at 70 bar, the pressure ratio is observed to be higher compared to the dry case for the whole

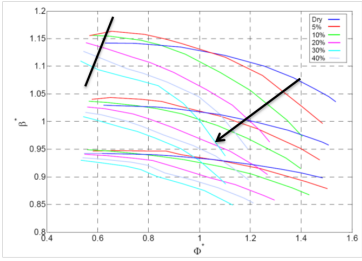

Figure 1: Change in range. Compressor pressure ratio versus flow rate for three different motor speeds, n=20′000, 25′000, 30′000 rpm. The mixture is air and water at ambient conditions as inlet conditions and the plot axes are normalized. The picture is taken from Fabrizzi et al. [5]

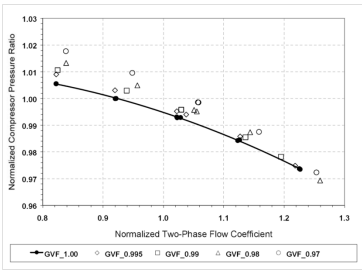

Figure 2: Normalized compressor pressure ratio as a function of Gas Volume Fraction for natural gas at a suction pressure of 70 bar, GVF = 0.995, 0.99, 0.98, 0.97 correspond to LMF=5.5%, 10.5%, 19%, 26%, respectively. The diagram is from Brenne et al [3]

operating range, see figure 2. The reason for the increase in pressure ratio for the wet gas flow, compared to the dry gas flow, can be explained by the increase in flow density and intercooling of the gas phase by evaporation of the liquid phase. A lower suction temperature leads to a lower volume flow, which allows compression of a higher volume flow rate. This gives a lower discharge temperature and a higher discharge pressure. For a low suction pressure, the losses are higher than the above described effects, leading to a lower pressure ratio compared to the dry gas case. For higher pressure levels, the two-phase flow gains from the liquid phase and the pressure ratio is higher compared to the dry case.

Wet Gas Model

The wet gas model is based on a two step correction. The correction parameters contain non-dimensional numbers like the gas volume fraction, the gas mass fraction and the Reynolds number. In the first step, the reduction of the maximum flow is modelled by a correction to earlier choke on the stage characteristics. This is performed with a parameter depending on the liquid volume fraction. The increase in pressure and power are considered in the second correction step. Two versions are developed. In the first version, the change in discharge pressure is considered with a correction parameter, which is based on an often used correction model for two-phase flow in pipes. The power is calculated with the increase in mass, due to the liquid phase. The second correction version is based on the philosophy that there are more losses and an increased shaft power in the compression process.

The two versions give similar results. The shaft power for the wet gas compression is increased compared to the dry gas case. Also the pressure ratio is increased. The maximum flow is reduced for both versions. However, version 2 gives a steeper curve.

Further Investigations

The model of today is dependent on non-dimensional parameters, which are independent of the time. To extend the model for evaporation over the compression process, would be of interest. Liquid droplets at the compressor discharge indicate that not all the liquid is evaporated. This would give a time-dependent and more complex model. To model the interaction between the liquid droplets and the gas flow more detailed, is a further implementation step. For this correction step, the interaction between the liquid and the gas is proposed to be further investigated. To be able to make the wet gas model more general, different wet gas compression processes needs to be analysed and interpreted to the model.

Summary
In a wet gas compression process, well stream gas is compressed without pre-separation. The compression unit is smaller and lighter than a standard compression unit. Wet gas is defined as a gas with a liquid volume fraction of up to 5% within the oil and gas industry. The liquid phase introduces new physical processes to the gas.

When compressing a wet gas, the required power increases and the maximum suction flow may be significantly reduced. Smaller maximum flow means a smaller operating range and steeper compressor curves. The pressure ratio is different depending on wet gas mixture and suction conditions. For an air/water mixture at 1 bar, the pressure ratio for the wet gas compression is in general lower compared to the dry case, while the pressure ratio for a hydrocarbon mixture at 70 bar is higher. The effect on the pressure ratio can be explained by the change in flow density and intercooling effects on the gas phase.

The wet gas model is a first step and is based on multiphase flow in pipes. The wet gas model is divided into two correction steps. The first step considers the decreased maximum flow. The second step considers either the increase in pressure ratio or the increase in shaft power and increased losses. To correct the shaft power and the losses, a steeper curve is received.

For the future, an extension of the model for the evaporation process through the compressor and further investigations on the interaction between the liquid and the gas phase is suggested. Analyses of experiments for different machines and wet gas mixtures are proposed to be investigated. This would give a wider knowledge of what effect a wet gas have on the compressor performance for several different cases.

References

[1] T. Knott. *"Subsea gas feels the pressure"*. Upstream Technology, vol. Q2, no. Q2, pp. 12-25, 2013.

[2] M. Chesshyre.*"Åsgard's case for subsea gas compression"*. Off-shore Engineer, no. December, pp. 50-51, 2010.

[3] L. Brenne, T. Bjoerge, J.L. Gilarranz, J.M. Koch, H. Miller,*"Performance evaluation of a centrifugal compressor operating under wet gas conditions"*. Texas, Houston: 34th Turbomachinery composium: 2005.

[4] L. Brenne, T. Bjoerge, L. E. Bakken, Øyvind Hundseid,*"Propspects for sub sea wet gas compression"*. Berlin, Germany, ASME Turbo Expo, GT2008-51158, 2008.

[5] M. Fabbrizzi, C. Cerretelli, F. Del Medico and M. D'Orazio, *"An experimental investigation of a single stage wet gas centrifugal compressor"*. Orlando, Florida, USA, ASME Turbo Expo, GT2009-59548, 2009.

Nomenclature

Variables

A	m^2	area
a	m/s	speed of sound
α	m^2/s	thermal diffusivity
C	–	flow dependent constant
c	m/s	absolute velocity
c_d	–	drag coefficient
c_p	kJ/(kg K)	specific heat constant at constant pressure
CorrPar1, CorrPar2	–	correction parameter
D	m	diameter
δ	–	density ratio
E	kJ	energy
ε	–	void fraction
ϵ	–	relative error
η	–	efficiency
f	–	friction factor
Fr	–	Froude number
G	kg/(s m^2)	mass flux
g	m/s^2	gravitational acceleration
GMF	–	gas mass fraction
GVF	–	gas volume fraction
H	kJ	enthalpy
h	kJ/kg	enthalpy
HTC	W/(m^2 K)	heat transfer coefficient
L	m	characteristic length
λ	W/(m K)	thermal conductivity
LMF	–	liquid mass fraction
LVF	–	liquid volume fraction
m	kg	mass
$\dot{m}$	kg/s	mass flow rate
Ma	–	Mach number
N	1/min	rotational speed
n	–	polytropic constant
Nu	–	Nusselt number
μ_d	Pa s=N s/m^2	dynamic viscosity
μ_y	–	pressure coefficient, polytropic head coefficient
μ_0	–	power coefficient, work input coefficient
P	W	power
p	bar=10^5 Pa	pressure
Pr	–	Prandtl number
Φ	–	multiplier
$\phi = \frac{\dot{V}}{D^2 \cdot u_2}$	–	flow coefficient

Continued on next page

Table 1 – *Continued from previous page*

π	–	pressure ratio
ψ_B,λ_B	–	constants for Baker diagram
Q	W	internal heat transfer
q	bar=10^5 Pa	dynamic pressure
R_i	kJ/(kg K)	specific gas constant
Re	–	Reynolds number
ρ	kg/m^3	density
ρ_h	kg/m^3	homogenous density
σ	N/m	surface tension
T	K	temperature
u_2	m/s	circumferential velocity/impeller tip speed
$\bar{u}$	m/s	mean velocity
u_s	m/s	superficial phase velocity
V	m^3	volume
$\dot{V}$	m^3/s	volume flow rate
$\upsilon = \frac{\mu_d}{\rho}$	m^2/s	kinematic viscosity
W	kJ	work
w	m/s	relative velocity
We	–	Weber number
X	–	Lockhart-Martinelli parameter
x	–	place holder
Z	–	compressibility, real gas factor
z	m	height indicator

Subscripts

1	suction/inlet
2	discharge/outlet
a	air/acceleration
c	calculated
d	dynamic
D	drag
f	friction
G	gas
h	homogeny
i	specific
is	isentropic
L	liquid
m	measured
pol	polytropic
Sh	shaft
St	static
v	volume
W	water
w	wet

Definitions

dry gas	gas without a liquid phase
wet gas	gas with a liquid phase
be aware:	there are different definitions of dry and wet gas found in literature

Contents

1 Introduction

The first chapter introduces the topic wet gas compression, gives the scope of this work and the outline of the report is described.

1.1 Background

The investigations on wet gas compression have a history of more than thirty years. In the beginning the goal was to understand if compression of a wet gas was possible and if it was profitable. Today, the oil and gas industry puts a big interest in reducing the size of the compression unit, since many gas fields are located far away from land in deep water. This means difficulties and high expenses to build a platform with a standard compression unit. The pressure in a gas reservoir decreases over time, which means that the gas production declines and in the end ceases, according to T. Knott [1]. M Chesshyre [2] writes that by placing a compression unit directly on the shore bed, as close to the source as possible, the production life can be further extended, since the compression process contributes with benefits like a stable and high gas flow rate and enhancement of the overall recovery.

In a standard compression process, the gas and the liquid phase are separated in a separator before compression. Each phase is thereafter compressed; the gas in a compressor and the liquid in a pump. After the compression, the liquid and the gas phases are mixed again and transported to surface facilities where the flow is processed.

In a wet gas process, the separator and the pump are replaced by a slug catcher and there is no separation of the two-phases. The liquid and the gas phase flow both through the compressor.

Wet gas compression allows for smaller foot-print and reduction of the weight by replacing heavy and space-consuming units such as separators by a slug catcher [3]. Furthermore, no pump is required. The incoming wet gas is, thereafter, compressed in a multiphase boosting unit without phase separation.

A wet gas compression unit, typically, needs to manage a compression of a wet gas with liquid volume fraction up to 5 %, be robust and able to handle corrosive liquids and gases, which increase erosion and corrosion on the machine. To minimize defects during the compression process, it is of favour if the design is as simple as possible, due to unmanned operation under water. The unit also needs to be able to work under variable conditions, such as variations in liquid mass fraction or suction pressure levels.

Alternatives such as radial compressors, contra rotating axial compressors and positive displacement screws are investigated in literature, but Brenne et al [4] states that the focus is on radial compressors due to its robustness, high volume flow capacity and traditional usage within the oil and gas industry.

1.2 Scope of the Work

During the Master Thesis at MAN, the thermodynamic performance of a radial compressor working under wet gas conditions is investigated.

To achieve the target a literature study is performed to get an overview over what is done within the area wet gas and wet gas compression. A literature research is also achieved to understand the physics. Measurement data for a wet gas compression test campaign is analysed and an extended compressor prediction model from dry gas to wet gas is developed. The extended gas model is calibrated with measurement data.

The analyse of the measurement data is excluded from this public version of the Master Thesis report.

1.3 Structure of the Report

The report is divided into 5 chapters. The first chapter includes the aim of the Master Thesis, an introduction to the topic handled and the structure of the report.

Chapter 2 describes basic equations and provides derivations for the thermodynamic modelling of compressors and wet gas, including the dynamics of different types of flow regimes and flow maps are clarified.

Literature studied and observations made by others are presented in Chapter 3.

The results of the modelling are presented in Chapter 4. A dry gas model for the thermodynamic modelling of the compressor and a wet gas model are

presented and the agreement with the observations is discussed.

Chapter 5 summarizes the results and gives conclusions. Furthermore, an outlook on possible future work is included.

In the end of the report, the acknowledgement, the bibliography and the appendix can be found.

2

Basics about Compressors and Wet Gas

This chapter serves as an introduction to the topic of thermodynamic modelling of radial compressors and wet gas flows. Important equations, relations and definitions for turbomachinery and wet gas flow are explained.

2.1 Thermodynamics of a Radial Compressor

Radial compressors, also referred to as centrifugal compressors, are often used for natural gas pipelines, due to their advantages in size, operating range and robustness. Saravanamutto et al. [5] state that a radial compressor is shorter compared to an axial compressor. The radial compressor has a better resistance to foreign object damage and less resistance in loss of performance by built-up of deposits on impeller surfaces compared to an axial compressor. Radial compressors are also known for being able to operate during a wider range of volume flow at given rotational speed.

As written by Lüdkte [6], radial compressors are suitable for operation with gas production, hydrocarbon processing and chemical processing. When compressing different types of real gases, a stage mismatching from the first to the last stage appears as a consequence of the real gas. A stage mismatching can reduce the head, efficiency and operating range of the compressor substantially.

A cross-section of a radial compressor can be seen in Figure 2.1, taken from Lüdtke [6]. The working fluid is lead into the compressor suction (A) and into the impeller (C), where rotational and centrifugal forces act on the gas. To decrease the discharge velocity and to receive a further increase of pressure, a diffuser (D) is used. The bend (E) and the return blading (F) lead to the next stage. After the last stage, a volute (K) is used to collect the compressed fluid and lead it to the diffuser (L) in the compressor exit. The compressor process ends in the discharge nozzle (M). The purpose of the impeller is to increase the energy level of the fluid by whirling it outwards, which means that the angular momentum of the fluid is increased. An increase in static pressure is also received [5]. The diffuser is used to convert

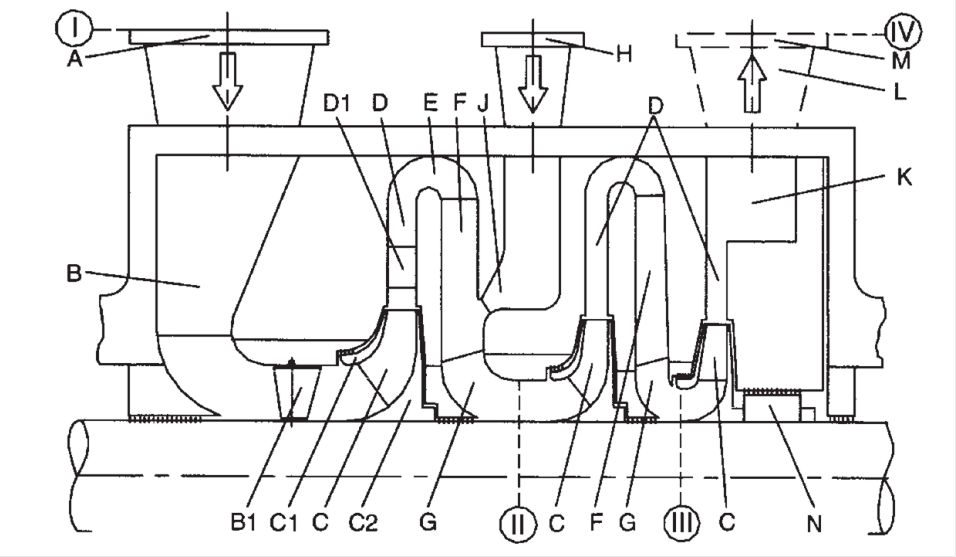

Figure 2.1: A cross-section of a radial compressor. A: Compressor suction. C: Impeller. D: Vaned diffuser. E: Return bend. F: Return vane channel. G: Bend. K: Volute. L: Exit diffuser. M: Discharge nozzle. The picture is taken from Lüdtke [6]

the kinetic energy into pressure energy, as described by e. q. Dixon et al. [7]. The velocity of the fluid is decelerated and the remaining rise in static pressure is received. The compression process of a centrifugal compressor is affected by both axial and radial forces to compress the fluid to a higher pressure.

To be able to explain the enthalpy rise in the impeller, the first law of thermodynamics is introduced. If a system containing a closed loop is taken through a complete cycle, the supplied heat is equal to the work done, as stated by Dixon et al. [7]. From state 1 and state 2, a change in energy within the system is received.

$$E_2 - E_1 = \int_1^2 (dQ - dW) \tag{2.1a}$$

where E_2 and E_1 are the energy of the two states, Q is the heat transfer and W is the work done. The energy of a state for an open system is

$$E = H + \frac{1}{2} \cdot m \cdot c^2 + m \cdot g \cdot z \tag{2.2a}$$

where H is the enthalpy, m is the mass, c is the absolute velocity, gz is the potential energy per unit mass. By combining equation (2.1) and equation (2.2)

$$P + \dot{Q} = \dot{m} \cdot (h_{St_2} - h_{St_1} + \frac{c_2^2 - c_1^2}{2} + g \cdot (z_2 - z_1)) \tag{2.3a}$$

where P is the positive power, Q is the rate of the heat transfer from the surroundings to the control volume, h_{St} is the specific static enthalpy and $\frac{1}{2} \cdot c^2$ is the kinetic energy per unit mass. The potential energy difference between suction and discharge is negligible for a compressor. This means that the total enthalpy simplifies to

$$h = h_{St} + \frac{c^2}{2} \tag{2.4a}$$

The heat loss of the gas to the environment is typically less than 1 % of the energy input and can therefore be neglected [6]. The *required power* P for the compression process is thermodynamically written as

$$P = \dot{m} \cdot (h_2 - h_1) = \dot{m} \cdot \Delta h \tag{2.5a}$$

The enthalpy rise produced by a centrifugal compressor can be expressed by the *blade tip speed* u_2, which can be written as the product of the *rotational speed of the impeller* N and the *impeller diameter* D_2

$$u_2 = N \cdot \pi \cdot \frac{D_2}{2} \tag{2.6a}$$

The enthalpy rise in a compressor stage can be given as the change in impeller tip speed and the *relative velocity* w for the inlet and the outlet of the compressor

$$h_2 - h_1 = \frac{1}{2} \cdot (u_2^2 - u_1^2) + \frac{1}{2} \cdot (w_1^2 - w_2^2) \tag{2.7a}$$

The first term on the right hand side is explained by Dixon et al. [7] as the contribution from the centrifugal action caused by the change in radius. The second term expresses the contribution from the diffusion of relative velocity.

The specific work done on the fluid in a centrifugal compressor is explained by *Euler's work equation*

$$\Delta P = u_2 \cdot c_{\theta 2} - u_1 \cdot c_{\theta 1} \tag{2.8a}$$

If the flow going at the impeller eye of the compressor stage has no whirl component or angular momentum the *absolute tangential velocity* c_1 is zero and Euler's work equation simplifies to

$$\Delta P = u_2 \cdot c_{\theta 2} \tag{2.9a}$$

The *flow coefficient* ϕ for turbomachinery is commonly calculated as the *volume flow* $\dot{V}$ at the compressor suction in stagnation condition normalized by the *impeller diameter* D_2 and the *impeller tip speed* u_2.

$$\phi = \frac{\dot{V}}{D_2^2 \cdot u_2} \tag{2.10a}$$

The *pressure ratio* π is the ratio of discharge and suction pressure of the compressor

$$\pi = \frac{p_2}{p_1} \tag{2.11a}$$

The *equation of state* for a real gas relates pressure p, volume flow $\dot{V}$, mass flow $\dot{m}$, temperature T, *specific gas constant* R_i and *compressibility factor* Z, as for example described by Cengel and Boyles [8]

$$p \cdot \dot{V} = \dot{m} \cdot R_i \cdot T \cdot Z \tag{2.12a}$$

Lüdtke [6] defines the *polytropic change of state* Δh_{pol} as the constant ratio of isentropic density change performed by small compression steps over the process, see illustration in Figure 2.2.

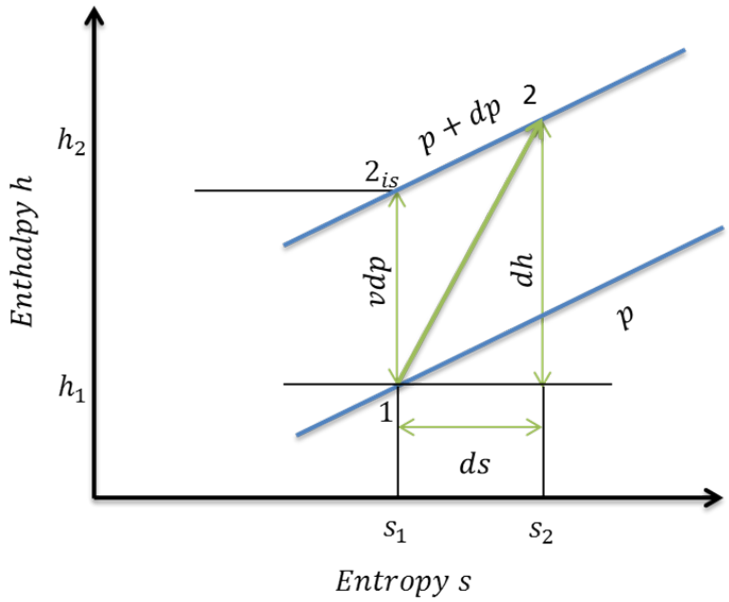

Figure 2.2: Illustration of a small compression step of the polytropic compression

The *polytropic head* Δh_{pol} is

$$\Delta h_{pol} = \int_{p_1}^{p} v dp \tag{2.13a}$$

given the integration follows the polytropic compression and each compression step has the same efficiency.

A derivation of the polytropic head for a perfect gas is shown below. Polytrophic relation according to Cengel and Boyles [8] is as follows

$$p \cdot v^n = const \rightarrow p_1 \cdot v_1^n = p_2 \cdot v_2^n \rightarrow v = v_1 \cdot (\frac{p_1}{p})^{\frac{1}{n}} \tag{2.14a}$$

where n is the *polytropic exponent*. By rearranging equation (2.14) and knowing the start and end conditions in the focus area the polytropic constant can be calculated.

$$n = \frac{\ln(\frac{p_1}{p_2})}{\ln(\frac{v_2}{v_1})} \tag{2.15a}$$

By combining equation (2.13) and equation (2.14), the polytropic head for a perfect gas is

$$\Delta h_{pol} = \int_{p_1}^{p_2} v_1 \cdot (\frac{p_1}{p})^{\frac{1}{n}} dp = \int_{p_1}^{p_2} v_1 \cdot p_1^{\frac{1}{n}} \cdot p^{-\frac{1}{n}} dp \tag{2.16a}$$

$$\Delta h_{pol} = v_1 \cdot p_1^{\frac{1}{n}} \cdot (1 - \frac{1}{n}) \cdot [{p_2}^{\frac{n-1}{n}} - {p_1}^{\frac{n-1}{n}} =\rightarrow \tag{2.16b}$$

$$\frac{n-1}{n} \cdot [{p_2}^{\frac{n-1}{n}} \cdot v_1 \cdot p_1^{\frac{1}{n}} - v_1 \cdot {p_1}^{\frac{n-1}{n}+\frac{1}{n}}] =\rightarrow \tag{2.16c}$$

$$\frac{1-n}{n} \cdot [p_2 \frac{1-n}{n} \cdot v_1 \cdot p_1 \frac{1}{n} - v_1 \cdot p_1] \tag{2.16d}$$

$$\Delta h_{pol} = \frac{n-1}{n} \cdot (p_2 \cdot v_2 - p_1 \cdot v_1) \tag{2.17a}$$

For a real gas, a simplified approach to compute the change in polytropic height is derived. The polytropic change of state is

$$p \cdot v_v^n = const \tag{2.18a}$$

The *polytropic volume exponent* n_v is defined at constant polytropic efficiency by the ratio of the pressure and the specific volume

$$n_v = -\frac{v}{p} \cdot (\frac{\delta p}{\delta v})_{\eta_{pol}} \tag{2.19a}$$

A derivation of the polytropic volume exponent can be seen in the book written by Lüdtke [6]. The polytropic head for a real gas with a simplified approach is shown

$$\Delta h_{pol} = \int_{p_1}^{p} v dp = Z_1 \cdot R \cdot T_1 \cdot \frac{n_v}{n_v - 1} \cdot ((\frac{p_2}{p_1})^{\frac{n_v-1}{n_v}} - 1) \tag{2.20a}$$

The *polytropic efficiency* $_{pol}$ for a real gas is with a simplified approach for the inlet conditions shown

$$\eta_{pol} = \frac{\Delta h_{pol}}{\Delta h} = \frac{\int_{p_1}^{p} v dp = Z_1 \cdot R \cdot T_1 \cdot \frac{n_v}{n_v-1} \cdot ((\frac{p_2}{p_1})^{\frac{n_v-1}{n_v}} - 1)}{\Delta h} \tag{2.21a}$$

The polytropic efficiency for a perfect gas depends on the polytropic volume exponent and the inlet and outlet conditions. For a wet gas, the discharge conditions are hard to calculate. Therefore, approximations about the discharge conditions usually have to be done. The polytropic efficiency is used

when evaluating a compressor, since this efficiency is calculated in many small steps over the process.

The *work input coefficient* μ_0 indicates the specific power input of a compressor stage and is defined as

$$\mu_0 = \frac{\Delta h}{u_2^2} \tag{2.22a}$$

The *polytropic head coefficient* μ_y of a compressor stage is the polytropic head over the impeller tip speed.

$$\mu_y = \frac{\Delta h_{pol}}{u_2^2} \tag{2.23a}$$

2.2 Dimensionless Numbers

The *Reynolds number Re* is one of the most powerful parameters in fluid dynamics, according to Anderson [9]. The Reynolds number helps predicting similar flow patterns in different fluid flow situations. It is, for example, used to predicting whether the turbulence behaviour of a flow around two geometrical alike bodies is the same. The number is defined as the ratio of the inertia force over the viscous or friction force, see definition from for example Lüdtke [6].

$$Re = \frac{\rho \cdot \bar{u} \cdot L}{\mu_d} = \frac{\bar{u} \cdot L}{\upsilon} = \frac{\dot{m}}{\frac{\pi}{4} \cdot D \cdot \mu_d} \tag{2.24a}$$

where ρ is the density, $\bar{u}$ is the mean velocity, L is the characteristic length, μ_d the dynamic viscosity. υ is the kinematic viscosity, $\dot{m}$ is the mass flow rate and D is the diameter.

For oil and gas applications, the Reynolds number in a pipe is usually so large that an assumption of turbulent flow in the pipe can be taken.

The *Prandtl number Pr* is defined by Anderson [9] as the ratio between the *kinematic viscosity* υ and *thermal diffusivity* α. Anderson explains the number as a ratio of energy dissipated by friction to the energy transported by thermal conduction.

$$Pr = \frac{\upsilon}{\alpha} = \frac{c_p \cdot \mu_d}{\lambda} \tag{2.25a}$$

Where υ is the kinematic viscosity, α the thermal diffusivity, c_p is the specific heat capacity for a constant pressure and λ thermal conductivity.

The parameters defining the Prandtl number are material properties; indicate that the Prandtl number can be used to analyse gases, as stated by Anderson [9].

The Prandtl number is used to compare the velocity boundary layer with the thermal boundary layer. The relations for the number are according to Anderson [9] as follows.

- $\mathrm{Pr} > 1$ the velocity boundary layer is bigger than the temperature layer
- $\mathrm{Pr} = 1$ the boundary layers are equal
- $\mathrm{Pr} < 1$ the temperature boundary layer is bigger than the velocity boundary layer

The *Nusselt number Nu* is the ratio between *convective* and *conductive heat transfer*, described by Sundén [10]. The convective heat transfer is the transfer of energy between a solid surface and a fluid in motion. The conductive heat transfer occurs in the solid perpendicular to the surface, according to Cengel and Boyles [8].

$$Nu = \frac{convecive heat transfer}{conductive heat transfer} = \frac{HTC \cdot L}{\lambda} \tag{2.26a}$$

The Nusselt number is used to compare the thermal resistance in a solid with the heat transfer to the gas. A Nusselt number close to one means a similar convective and conductive heat transfer.

The *Weber number We* can be used when analysing liquids in gases, for example analysing droplet formation and atomization of liquids, according to VDI Wärmeatlas [11].

$$We = \frac{\rho \cdot u^2 \cdot L}{\sigma} \tag{2.27a}$$

It is a ratio between the inertia of a fluid and its *surface tension* σ.

The *Froude number Fr* is defined by von Böckh [12] as the ratio between the inertial and the gravitational force.

$$Fr = \frac{v}{c} = \frac{v}{\sqrt{L \cdot g}} \tag{2.28a}$$

Where v is the velocity, g is the gravitational acceleration and L is the characteristic length.

The Froude number is used for analysing the flow in a channel similar to a river and to study the wave resistance between different types of bodies.

- $\mathrm{Fr} < 1$ means a subcritical flow. At low flow rates, disturbances in the system travel upwards in the system, indicating that it is the circumstances downstream, which control the flow, according to Endress+Hauser Flowtec AG [13]. When the number is below one, the gravitation force has a big impact on the flow and there is a risk for stratified flow, according to VDI Wärmeatlas [11].

- Fr $>$ 1 means a supercritical flow. Disturbances upstream in the system will travel downstream in the system, indicating it is the conditions upstream, which control the system.
- Fr $=$ 1 means a critical flow, leads to an unstable flow. According to Endress+Hauser Flowtec AG [13], the surface seems to be calm, but the main flow move downwards.

Mostly, this number is used to analyse the flow in a channel, for example a river, or testing of ships, according to VDI Wärmeatlas [11]. A liquid and a gas Froude number is used in the flow maps for multiphase flows in pipes.

The *Mach number Ma* is the velocity v divided by the local speed of sound a, as defined by for example Dixon and Hall [7],

$$Ma = \frac{v}{a} \tag{2.29a}$$

The author explains the local speed of sound for a perfect gas as a function of the *gas constant* R_i, *local temperature* T and *isentropic expansion constant* γ. For a real gas the speed of sound is dependent on the *compressibility factor* Z, too

$$a = \sqrt{\gamma \cdot T \cdot R_i \cdot Z} \tag{2.30a}$$

2.3 Wet Gas Flow

This chapter introduces to the wet gas flow, which is well studied for pipe flow and flow elements such as bends and orifices. Basic equations and derivations as well as basics concerning wet gas flow are introduced.

2.3.1 Basics about Wet Gas Flow

A *phase* is a thermodynamic definition for the state of the matter. A phase can either be *solid*, *liquid* or *gas*. For a multiphase flow, several phases flow simultaneously. A two-phase flow is described as a flow with two-phases flowing together in for example a pipe, according to Hetsroni [14]. A two-component flow describes the flow of two chemical substances. A wet gas can be explained as a two-phase flow since the flow mainly contains a liquid and a gas phase. When the wet gas mixture contains sand too, the flow can be called a three-phase flow.

A multiphase flow is in *thermal equilibrium* when the temperatures of the phases are equal. For the suction side of the compressor, it is possible to say that the mixture is in thermal equilibrium, due to long suction pipelines. When going into the compression process, the liquid and the gas phase behave differently, depending on the characteristics of each phase. According to Ransom et al. [15], it is not possible to assume thermal equilibrium within the compressor, due to unpredictable evaporation and condensation in the

process.

According to a variety of sources [4], [15], [16], [17], a wet gas is described as a gas with a liquid volume fraction of maximum 5 %. For oil and gas application, this may lead to a liquid mass fraction of up to 70 % of the total mass flow, depending on the surrounding conditions. According to Bertoneri et al. [17], multiphase pumping is recommended for a mixture with a liquid volume fraction greater than 5 %.

2.3.2 Basic Equations

In a fluid flow, the *gas mass fraction GMF* and *liquid mass fraction LMF* describe the mass flow rate of each component compared to the total mass flow rate of the mixture, respectively, as given in following equations

$$GMF = \frac{\dot{m}_G}{\dot{m}_G + \dot{m}_L} \tag{2.31a}$$

$$LMF = \frac{\dot{m}_L}{\dot{m}_G + \dot{m}_L} \tag{2.31b}$$

The *gas volume fraction GVF* and *liquid volume fraction LVF* describe the volume flow of each phase compared to the total volume flow of the mixture, respectively.

$$GVF = \frac{\dot{V}_G}{\dot{V}_G + \dot{V}_L} \tag{2.32a}$$

$$LVF = \frac{\dot{V}_L}{\dot{V}_G + \dot{V}_L} \tag{2.32b}$$

As the liquid typically has lower velocities, the actual volume of the liquid in the pipeline and thus the cross-section blocked by the liquid might be significantly higher than the liquid volume fraction.

The *gas void fraction* ε_G and the *liquid void fraction* ε_L describe the volume or area occupied by each phase over a given volume of the flow or a given cross-sectional area

$$\varepsilon_G = \frac{V_G}{V_G + V_L} = \frac{A_G}{A_G + A_L} \tag{2.33a}$$

$$\varepsilon_L = \frac{V_L}{V_G + V_L} = \frac{A_L}{A_G + A_L} \tag{2.33b}$$

The void fraction differs from the volume fraction since the void fraction is taken for a specific area or volume and not for a flow.

The *density* ρ for a liquid or a gas can be calculated from the ratio of the mass and the volume flow rate:

$$\rho = \frac{\dot{m}}{\dot{V}} \tag{2.34a}$$

The *density ratio* δ, also called relative density according to Cengel and Boyles, [8], is defined as

$$\delta = \frac{\rho_G}{\rho_L} \tag{2.35a}$$

The density ratio is used to distinguish different types of flow in a pipe. Due to gravity force, *stratified flow* is more likely to occur in a pipe with a low density ratio.

In a variety of sources [3], [16], [18], the homogenous density is used for characterizing annular dispersed flows. As a simplification, the flow is then handled as a single phase gas

$$\rho_h = GVF \cdot \rho_G + (1 - GVF) \cdot \rho_L \tag{2.36a}$$

$$\frac{1}{\rho_h} = \frac{1 - GMF}{\rho_L} + \frac{GMF}{\rho_G} \tag{2.36b}$$

The homogenous density agrees with the average density in the pipe, only if all fluids travel with the same velocity.

The relation between the volume fraction and the mass fraction can be expressed by the density ratio

$$LVF = \frac{LMF}{LMF + \frac{1-LMF}{\delta}} = 1 - GMF \tag{2.37a}$$

The equation above shows that the mass fraction can be converted to volume fraction via the density ratio. By altering the pressure level, the density ratio changes. This impacts the liquid volume fraction, as can be seen in figure 2.3. The lines show different pressure levels, brown indicates on a low pressure and yellow a higher pressure level.

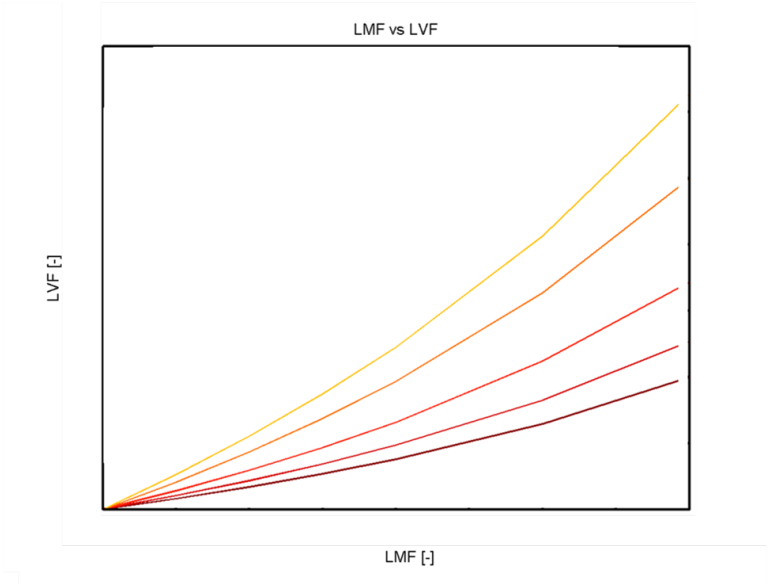

Figure 2.3: The change in liquid volume fraction for different liquid mass fractions and different pressure levels. Brown is low pressure level and yellow is high pressure level

2.3.3 Multiphase Flow Regimes

This chapter treats the subject flow regimes and flow maps. The flow regimes affect the pressure losses in multiphase pipelines as well as the performance of a wet gas compressor. The flow map indicates which flow regime is present for a certain pipe flow simulation.

Flow Regimes

Different types of flow regimes can emerge in a pipe with a two-phase flow. They mainly depend on the liquid and gas properties, such as *viscosity, surface tension, relative mass fractions, densities* and *flow velocities* as well as the orientation of the pipe. Different flow regimes are shown in Figure 2.4 and Figure 2.5, for horizontal and vertical flow, respectively.

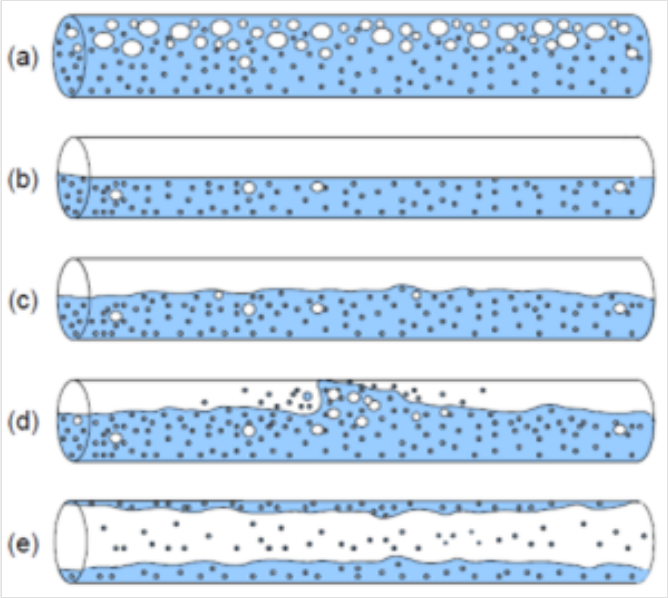

Figure 2.4: Different types of flow regimes for a horizontal pipe. The pipes from a) to e) shows: a) Bubble flow, b) Stratified flow, c) Wavy flow, d) Slug flow, e) Annular dispersed flow. Source: [19]

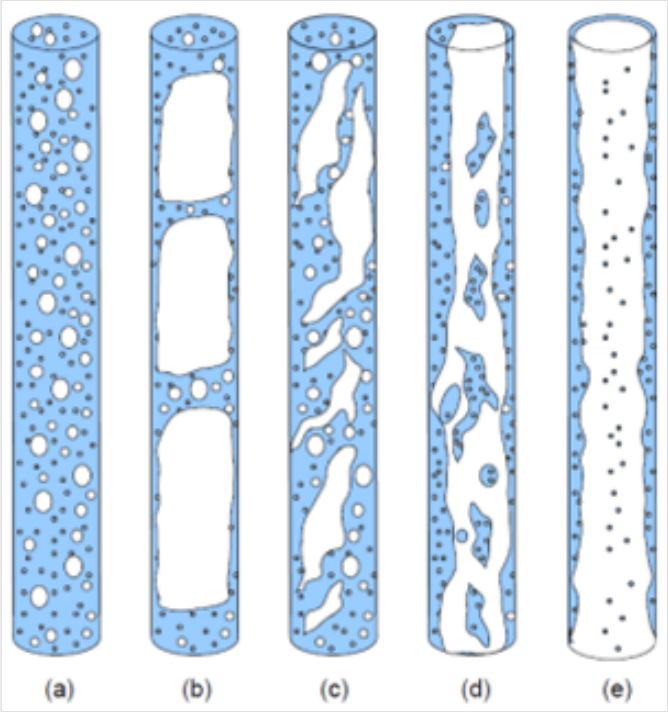

Figure 2.5: . Different types of flow regimes for a vertical pipe. The pipes from a) to e) shows: a) Bubble flow, b) Slug/plug flow, c) Foam flow, d) Annular streak flow, e) Annular dispersed flow. Source: [19]

The different flow regimes are defined according to von Böckh [12].

- *Bubble flow*
  Bubble flow arises for flows with low gas volume fraction. The flow is characterized of bubbles of gas flowing with the liquid flow.

- *Intermittent Slug and Plug flow*
  Slug and Plug flow are two-phase flows where the liquid and the gas phase flow separated. It is characterized by an unsettled flow with high waves, which obstruct the flow cross-section. The sizes of the obstructed sections are dependent on the flow gas content. Typical intermittent flows are

  - *Slug flow*
    Slug flow is characterized by sections with liquid which are interrupted by long bubbles of gas.
  - *Plug flow*
    Plug flow is characterized by sections with liquid and smaller gas bubbles than for slug flow.

- *Stratified flow*
  Stratified flow occurs for horizontal pipes only. The gas and the liquid phase flow vertically separated from each other in either a smooth or a wavy way, as described below.

  - *Smooth flow*
    The liquid and the gas phase flow separate from each other with a calm liquid surface, for example a calm lake without wind. Thus, the interaction forces between liquid and gas are minor.
  - *Wavy flow*
    For higher fluid velocities, the smooth liquid surface gets wavy and there is a rising interaction force between gas and liquid, for example a wavy river. If the velocity rises further, the wavy flow turns into slug or plug flow.

- *Annular dispersed flow*
  A two-phase flow with separation between the liquid and the gas phase. Most of the liquid phase flows as a layer on the pipe wall and the gas phase flows in the core with liquid droplets in between. Annular dispersed flow occurs for a flow with high gas velocity at high pressures and a low liquid content. The aerodynamic forces dominate the gravitational forces such that the heavier liquid spreads uniformly on the pipe wall.

- *Mist flow*
  The liquid phase flows as droplets in the gas flow. The mist flow regime occurs for high gas mass fraction and high velocity of the phases.

An observation from a variety of sources [16], [17], is that annular dispersed flow is a usual used assumption for multiphase flows in a compressor for upstream gas with higher pressures, due to high gas velocity, high gas density and low liquid volume fraction in the mixture. For annular dispersed flows, homogenous density is used to describe the density in a variety of papers [3], [16], [18]. The flow is then handled as a single phase flow.

Flow Map

A flow map is used to predict the flow regime for a multiphase pipeline flow. There are different ways of defining the axis in the diagrams and the areas of the flow regimes are usually predicted by measuring the flow for different conditions. An example of a flow map can be seen in Figure 2.6, where different gas/oil systems in horizontal pipes are evaluated. This type of flow map is also called *Baker diagram*. Usually, one axis describes a liquid/gas relation and the second axis describes the gas conditions.

There are three flow maps shown in this chapter. Figure 2.6 and 2.7 refer to horizontal flows, while Figure 2.8 refers to vertical flows.

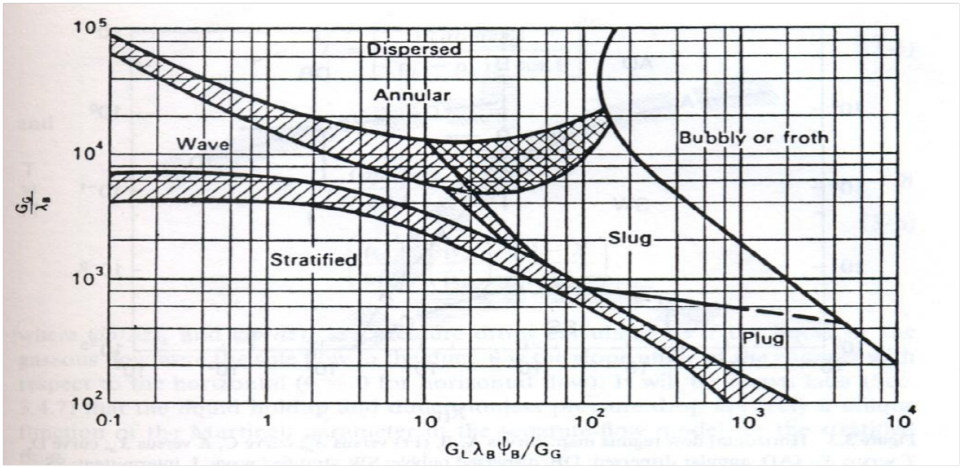

Figure 2.6: Flow map for a horizontal flow. The diagram is taken from [20]

The flow map shown in Figure 2.6 can be used for horizontal flows and different gas/oil systems. It is originally created by Baker in 1954 and has thereafter been modified by Scott, 1963. The diagram is called a Baker diagram. It is based on empirical data from a variety of sources, according to Tong and Tang [20].

The flow map is generated for air and water, but it can also be used for other gases and liquids. Their properties are taken into account by the

following two relations

$$\lambda_B = \sqrt{\frac{\rho_G}{\rho_a} \cdot \frac{\rho_L}{\rho_w}} \tag{2.38a}$$

$$\Psi_B = \frac{\sigma_w}{\sigma_L} \cdot (\frac{\mu_L}{\mu_w} \cdot (\frac{\rho_w}{\rho_L})^2)^{\frac{1}{3}} \tag{2.38b}$$

The x-axis shows a comparison of the *mass fluxes* between the liquid and the gas in the flow, while the y-axis shows the gas mass flux, according to Tong and Tang [20]. The mass fluxes are

$$G_G = \frac{\dot{m}_G}{A} \tag{2.39a}$$

$$G_L = \frac{\dot{m}_L}{A} \tag{2.39b}$$

The *area A* is described as the pipe cross-sectional area.

According to the flow map modified by Scott, a mixed flow with high gas content and high flow velocity would be plotted in the wavy stratified or dispersed annular flow region.

The flow maps shown in Figure 2.7 and Figure 2.8, horizontal and vertical flow, respectively, are developed by Shell Global Solutions, [21]. They are applicable for fully developed two-phase flows in equilibrium, typically after ten times the diameter of the pipe.

The axes show corrected Froude numbers. The x-axis shows a gas Froude number and the y-axis a liquid Froude number. The Froude number is a function of the *superficial phase velocity* u_{s_G}, u_{s_L}, density ratio and the feed pipe diameter. The superficial velocities do not represent the real gas and liquid velocities, but they are the velocity each phase would have if it flew alone in the pipe as given below.

$$u_{s_G} = \frac{\dot{V}_G}{\pi \cdot (\frac{D_{fp}}{2})^2} \tag{2.40a}$$

$$u_{s_L} = \frac{\dot{V}_L}{\pi \cdot (\frac{D_{fp}}{2})^2} \tag{2.40b}$$

The gas and liquid Froude numbers are

$$Fr_G = u_{s_G} \cdot \sqrt{\frac{\rho_G}{(\rho_L - \rho_G) \cdot g \cdot D_{fp}}} \tag{2.41a}$$

$$Fr_L = u_{s_L} \cdot \sqrt{\frac{\rho_L}{(\rho_L - \rho_G) \cdot g \cdot D_{fp}}} \tag{2.41b}$$

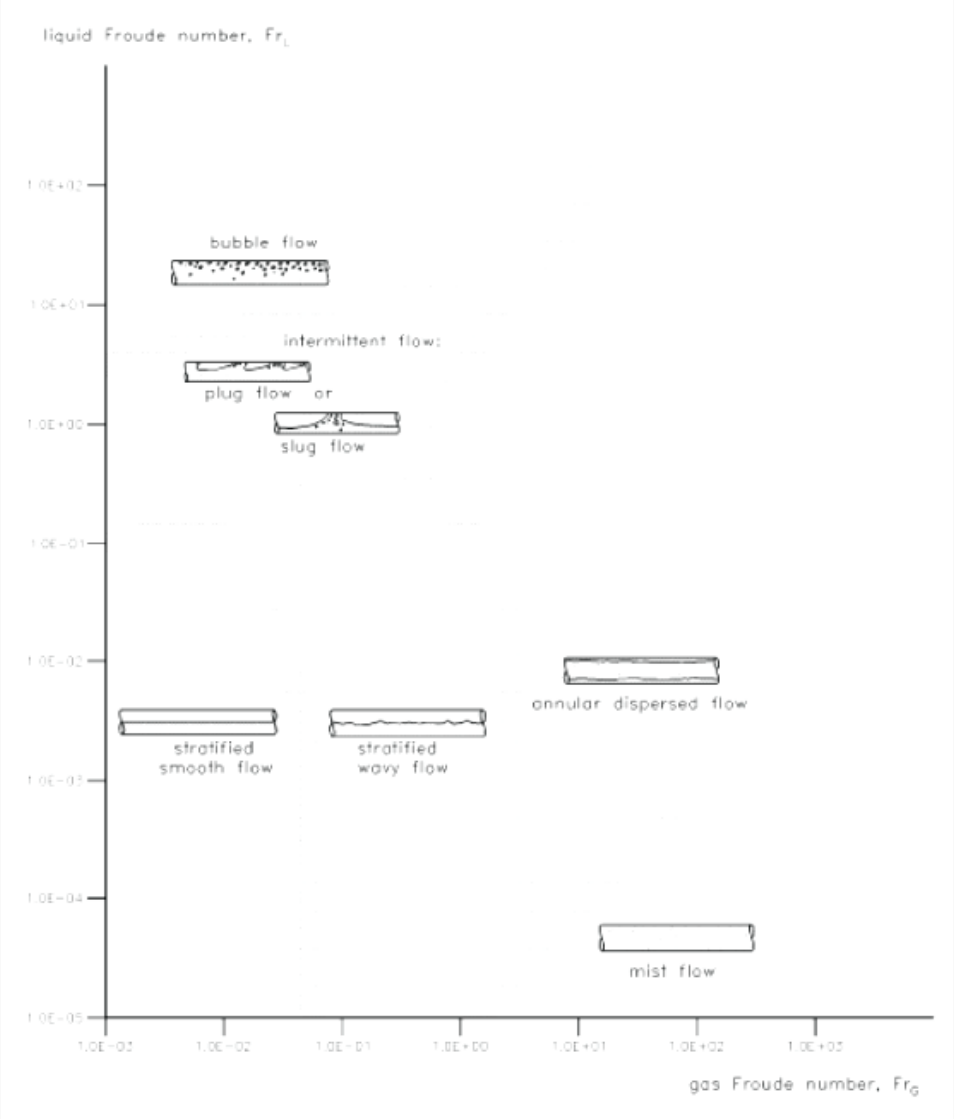

Figure 2.7: A flow map for a two-phase flow in equilibrium for horizontal feed pipes, taken from Shell Global Solutions [21]

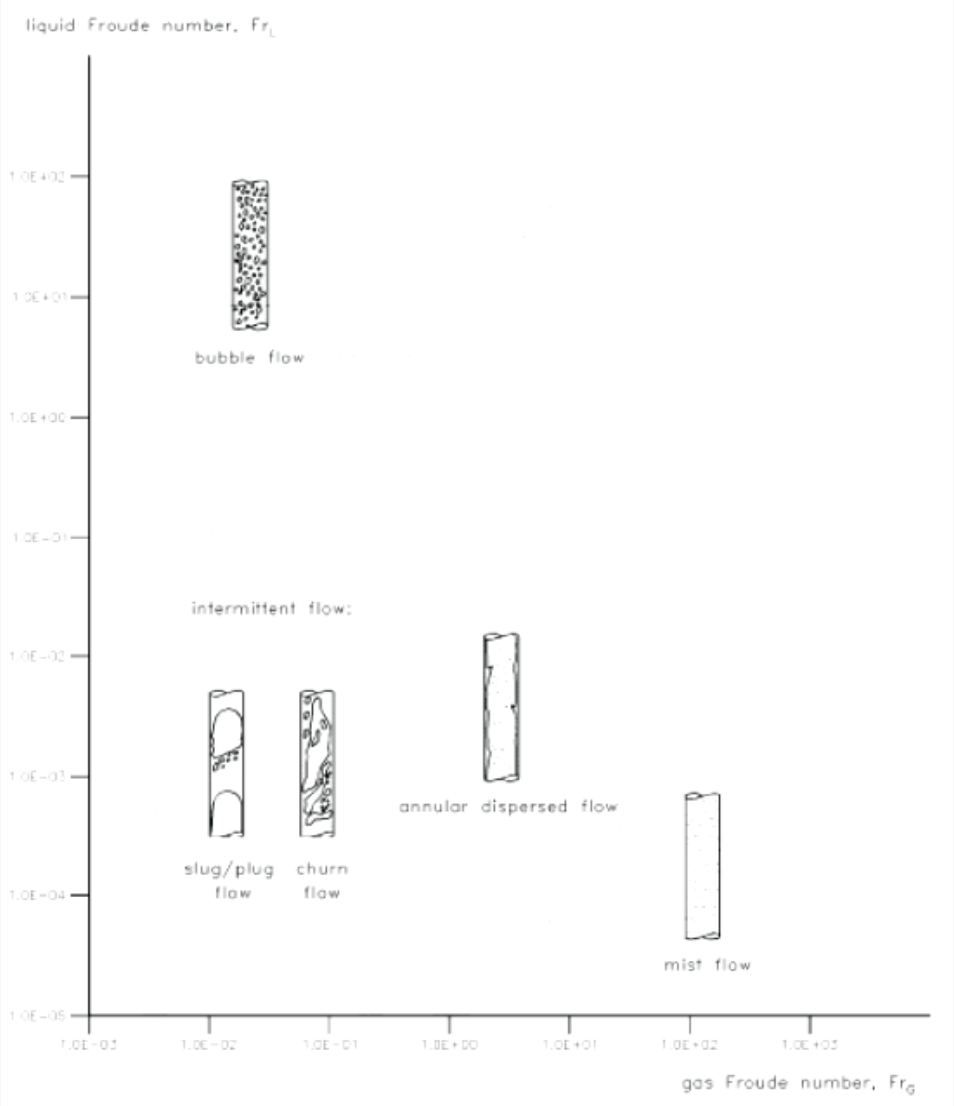

Figure 2.8: A flow map of two-phase flow in equilibrium for vertical feed pipes (up flow), taken from Shell Global Solutions [21]

2.3.4 Losses in a Loop

Description

Von Böckh [12] divides the pressure losses for multiphase flow into 3 components friction, hydrostatic and acceleration losses

$$\frac{dp}{dz} = (\frac{dp}{dz})_f + (\frac{dp}{dz})_a + (\frac{dp}{dz})_g \tag{2.42a}$$

Pressure losses occur through irreversible processes, as described by Cengel and Boyles [8]. To overcome the differences between a liquid and a gas phase, losses are introduced, where lost work converts to heat in the process. In an irreversible process, the heat produced by the friction work will not turn back to work and will therefore get lost.

According to Sundén [10], the pressure loss for fully developed flows in a channel is a function of *friction factor f*, length ratio, density and the mean flow velocity

$$\Delta p = 2 \cdot f \cdot \frac{L}{D} \cdot \frac{\dot{m}^2}{\rho} \tag{2.43a}$$

The friction factor for a straight pipe is depending on the Reynolds number. For high pressures and at high speeds, the expected flow within a compressor compressing wet gas is mist or annular dispersed flow, see Chapter 2.3.3. The annular dispersed flow is characterized by a liquid layer on the walls and impellers, with a dense droplet and gas flow in the core. The liquid layer leads to an increase in roughness, due to the waviness in the liquid layer and a more narrow flow path, due to the liquid accumulation, as written by Grüner et al. [16]. The mist flow is characterized by a dense droplet/gas flow, with increased losses mainly due to the difference in inertia of the droplet and gas and droplet impingement.

Friction losses is an irreversible process, which occurs when there is a momentum change between a gas and a liquid phase, a phase change or due to roughness in the boundary layer between the wall and the flow in a compressor.

Hydrostatic losses occur when there is a change in height, for example a vertical pipe according to von Böckh [12]. The hydrostatic losses are important to consider for the pipes both before and after the compressor, since the induced losses can cause a change in flow regime. A change in flow regime can have influence on the suction and surge conditions of the compressor.

When liquid droplets are accelerated by the gas flow, acceleration losses occur. According to Grüner et al. [16], the increase in acceleration losses occurs, due to acceleration of ejected droplets and liquid atomization. These do also result in a momentum loss. Liquid droplets have a higher inertia compared to gas. When liquid droplets are separated from the liquid layer,

the gas flow needs to overcome the inertia of the liquid droplet and this means acceleration losses. The release of droplets from the wall liquid layer will have an impact on the total flow and contribute to a dynamic pressure drop, according to von Böckh [12].

The size of the liquid droplets in a flow has an impact on the wet gas flow and on the interaction with the gas flow. Big droplets lead to a smaller drag coefficient and a higher Reynolds number. This means that the force needed to accelerate the droplet in the gas flow will be bigger, leading to increased pressure losses. The change in drag coefficient and Reynolds number is not constant, an increase in droplet diameter means a drag coefficient decrease of a factor two while it for the Reynolds number means an increase with a factor of three.

For low Reynolds numbers, the drag coefficient is high and the increase in drag coefficient is close to constant. This is called *Stokes flow*. According to VDI Wärmeatlas [11], the inertia forces on the particle can be neglected and paramount friction forces have an impact on the flow path of the droplet. The relation between the drag coefficient and Reynolds number can be seen in Figure 2.9. An increase in Reynolds number leads to a separation of the flow from the droplets and more turbulent flow. For a *Newton flow*, the drag coefficient is constant for increasing Reynolds number.

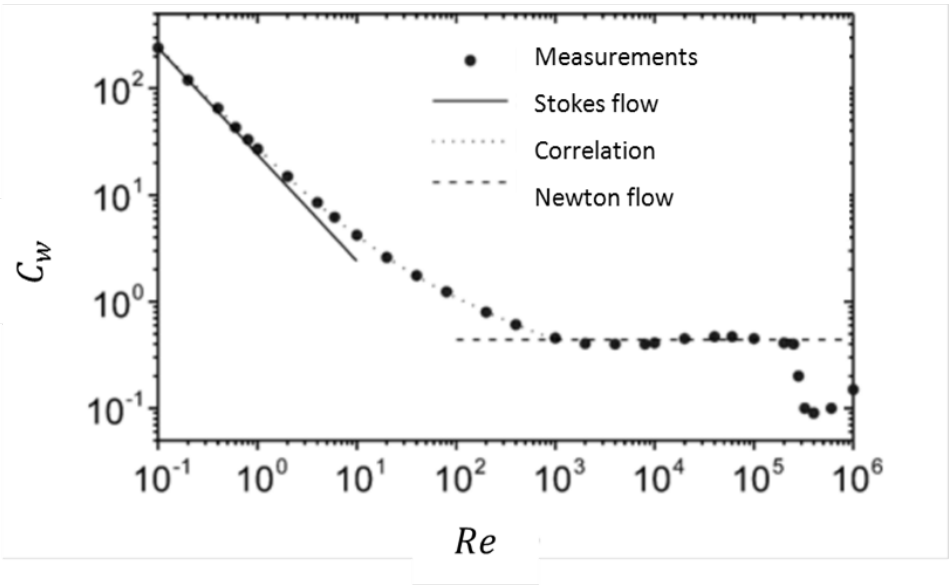

Figure 2.9: Variation of drag coefficient with Reynolds number for a sphere. Number 1 shows Stokes' theory [11]

The pressure drop in a pipe is a well-investigated topic by, for example, the nuclear business. It is important to know where changes in flow regime can occur, since this eases the prediction of where increased wear and tear

can occur in a pipe. The size of the pressure drop in a two-phase flow is different to the pressure drop in a single phase flow, according to VDI Wärmeatlas [11]. This is due to the change in mass of the flow, momentum and energy exchange. The interdependency between the liquid and the gas phase is dependent on the flow regime of the two-phase flow. For example, the momentum exchange in a slug flow can lead to big damages on a pipe.

Predicting

It is possible that the flow regime changes locally through the pipe. To be able to calculate whether there is a change in the pipe and the losses occurring, the effect on the performance of different flow models is described by a variety of authors [11], [14]. In this report a derivation of an often used pressure loss parameter is shown.

As described in chapter 2.3.4, the pressure drop is associated with friction, acceleration and gravity. An illustration of the introduced losses are shown in Figure 2.10. The friction losses in a pipe are dependent on the *wall shear stress* τ_0 and the cross-sectional area of the pipe A

$$(\frac{dp}{dz})_f = \frac{\tau_0 \cdot P}{A} \tag{2.44a}$$

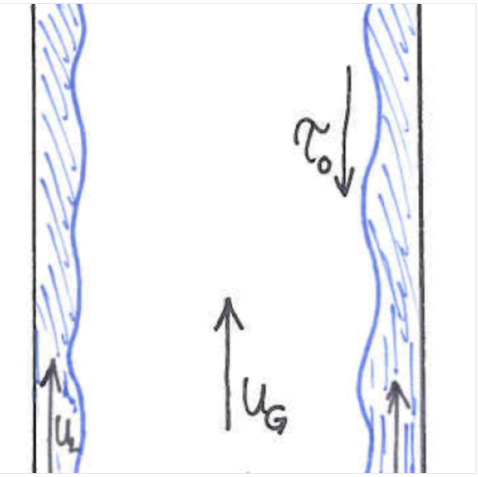

Figure 2.10: Illustration of the blockage and introduced roughness from the liquid phase in a pipe

Different ways to compute the losses for different types of flow regimes are reported by the VDI Wärmeatlas [11] and R. Hetsroni [14]. The flow can either be assumed to be homogenous or heterogeneous. For many of the pressure loss models in horizontal pipes, the losses due to acceleration and gravity are assumed to be negligible and the friction loss is the main factor to the pressure change.

With a homogenous model, the velocity of all phases in the flow are assumed to be equal. This gives a very simple prediction model, where the properties of the phases are averaged and is treated as a pseudo-fluid. The density of the homogenous flow is the sum of the mass fraction and density of each phase as described in equation (2.36)b.

The calculation process of the two-phase flow is as for a single-phase flow. The friction loss parameter from equation (2.42) is described by the liquid introduced *shear stress* τ_0, a *perimeter* P and the cross-sectional area of the pipe as described in equation (2.44). The equation (2.44) can be rewritten as

$$(\frac{dp}{dz})_f = \frac{2 \cdot f_{TP} \cdot \dot{m}^2}{D \cdot \rho_h} \tag{2.45a}$$

where f_{TP} is the friction factor of the two-phase flow, D is the diameter. The friction loss is the most complicated parameter to describe in a two-phase flow, according to Hetsroni [14]. The friction factor for a hydraulic smooth pipe is described as, independent on which phase,

$$f_{TP} = \frac{1}{4} \cdot \frac{0.3164}{Re^{0.25}} = \frac{1}{4} \cdot \frac{0.3164}{(\frac{\dot{m} \cdot D}{\mu})^{0.25}} \tag{2.46a}$$

with the *Reynolds number Re* as described in equation (2.24).

The pressure losses in a compressor can also be compared to pressure change for a sudden expansion. According to Hetsroni [14], the homogenous model gives more spread result than a heterogeneous model, which indicates that it is a heterogeneous model that should be used for the compressor prediction model.

For a heterogeneous model, the two-phases in the two-phase flow are considered to flow in the pipe as two separated streams with different velocities. The area of each phase are proportional to the gas void fraction ε_G, which is described in chapter 2.3.2. An illustration of the separated flow can be seen in Figure 2.10. The velocity of each phase is considered to be constant in any given cross-section within the zone occupied by the phase. However, the flow regime is not taken into account for modelling of a two-phase flow.

For a two-phase flow, the friction loss for the liquid phase is compared to the gas phase. For a hydraulic smooth pipe is the ratio between the two-phases

$$\frac{\frac{dp}{dz}L}{\frac{dp}{dz}G} = \frac{2 \cdot f_L \cdot \frac{\dot{m}_L}{\rho_L} \cdot \frac{L}{D}}{2 \cdot f_G \cdot \frac{\dot{m}}{\rho_G} \cdot \frac{L}{D}} \tag{2.47a}$$

By combining equation (2.46) with equation (2.47), the ratio of the losses

for a two-phase flow is

$$\frac{(\frac{dp}{dz})_L}{(\frac{dp}{dz})_G} = \frac{\frac{1}{4} \cdot \frac{0.3164}{Re_L^{0.25}}}{\frac{1}{4} \cdot \frac{0.3164}{Re_G^{0.25}}} \cdot \frac{\frac{\dot{m}_L}{\rho_L}}{\frac{\dot{m}_G}{\rho_G}} \tag{2.48a}$$

By deriving equation (2.48) and use equation (2.24) to describe the Reynolds number, the squared *Lockhart-Martinelli parameter* X is received

$$X^2 = \frac{\Delta p_L}{\Delta p_G} = \frac{\rho_G}{\rho_L} \cdot (\frac{\mu_L}{\mu_G})^{0.25} \cdot (\frac{1 - GMF}{GMF})^{1.75} \tag{2.49a}$$

The Lockhart-Martinelli parameter X is received from two-phase analyses performed by Lockhart and Martinelli in 1949 [14].

$$X = \sqrt{\frac{\Delta p_L}{\Delta p_G}} = (\frac{\rho_G}{\rho_L})^{0.5} \cdot (\frac{\mu_L}{\mu_G})^{0.1} \cdot (\frac{1 - GMF}{GMF})^{0.9} \tag{2.50a}$$

The Lockhart-Martinelli parameter is a function of the density ratio, which is pressure de-pendent and the viscosity ratio, which have a weak dependence.

Many pressure drop models for two-phase flow in pipes are based on the assumption that there is a higher liquid volume fraction than gas volume fraction in the flow. This is not the case for a wet gas flow where the liquid volume fraction is below 5 %. There are corrections depending on the liquid phase flow with corrections for the gas phase. In a wet gas flow, the correction parameters are for a gas phase flow with corrections for the liquid phase.

$$(\frac{dp}{dz})_f = \Phi_{TP}^2 \cdot (\frac{dp}{dz})_{f_{TP}} = \Phi_G^2 \cdot (\frac{dp}{dz})_{f_G} = \Phi_L^2 \cdot (\frac{dp}{dz})_{f_L} \tag{2.51a}$$

where Φ_{TP} is the two-phase multiplier, the Φ_G is the multiplier for the gas phase and the Φ_L is the multiplier for the liquid phase. Depending on whether it is a two-phase flow with a high liquid mass fraction or a two-phase flow with a high gas mass fraction, the multiplier is developed differently. There is one standard model developed by Chisholm in 1967, which can be used for predicting the losses for a flow with a high gas mass fraction

$$\Phi_G = 1 + C \cdot X + X^2 \tag{2.52a}$$

This multiplier can be used to calculate the losses in a two-phase flow

$$\Delta p_{TP} = \Phi_G^2 \cdot \Delta p_G = (1 + C \cdot X + X^2) \cdot \Delta p_G = \Delta p_G + C \cdot \sqrt{\frac{\Delta p_L}{\Delta p_G}} + \Delta p_L \tag{2.53a}$$

Where C is a constant depending on which flow regime is present in the two-phases. The constant C for a two-phase flow has following magnitudes

- 20 for a turbulent gas phase flow and a turbulent liquid phase flow

- 12 for a turbulent gas phase flow and a viscous liquid phase flow
- 10 for a viscous gas phase flow and a turbulent liquid phase flow
- 5 for a viscous gas phase flow and a viscous liquid phase flow

The multiplier takes following pressure losses into account

- Δp_G pressure losses for the gas
- $C \cdot \sqrt{\frac{\Delta p_L}{\Delta p_G}}$ pressure losses due to interaction between the phases
- Δp_L pressure losses introduced by the liquid phase only

The first term handles the gas losses, the second term additional losses due to the two-phase mixture of the flow and the third term handle the losses introduced by the liquid. When there is a small amount of liquid in the two-phase flow, the third term is negligible.

The Chisholm parameter for a flow with a high liquid mass fraction, a multiplier based on the pressure loss for the liquid phase is described

$$\Phi_G = 1 + \frac{C}{X} + \frac{1}{X^2} \tag{2.54a}$$

The two-phase flow for a flow with a high liquid fraction will be

$$\Delta p_{TP} = \Phi_L^2 \cdot \Delta p_L = \Delta p_L + C \cdot \sqrt{\frac{\Delta p_G}{\Delta p_L}} + \Delta p_G \tag{2.55a}$$

The first term on the right hand side describes the pressure losses for the liquid phase, the second term the pressure losses due to interaction between the phases and the last term describes the pressure losses due to the gas phase. For a flow with a high liquid volume fraction, the third term in equation (2.55) is negligible.

2.3.5 Mach Number Computation

The Mach number is affected by the liquid phase in a two-phase mixture. When the mixture is assumed to be compressible, the maximum flow velocity will be equal to the *speed of sound a* of the wet gas mixture. The speed of sound is described in equation (2.30).

The flow is assumed to be annular dispersed or mist flow, when there is a high pressure level and high gas content in the flow, as said in Chapter 2.3.3. Various papers apply homogenous density when there is an annular dispersed or mist flow. This density is applied when calculating the critical mass flow rate

$$\dot{m} = a \cdot A \cdot \rho_h \tag{2.56a}$$

According to von Böckh [12], the speed of sound or the critical velocity of a wet gas can be calculated with Laplace's equation. Studying a large gas volume fraction at isentropic conditions, the velocity of sound in two-phase flow can be described as

$$\frac{1}{a^2} = \frac{GVF}{a_G^2} \cdot (1 + (1 - GVF) \cdot (\frac{1}{\delta} - 1)) + \frac{1 - GVF}{a_L^2} \cdot (1 + GVF \cdot (\delta - 1)) \tag{2.57a}$$

As can be seen in Figure 2.11, the liquid impact of the gas on the speed of sound is strong. In this diagram an air/water mixture at 1 bar and 15 °C is studied. The liquid mass fraction is varied between 0 to 60 %. At given conditions, this mass fraction will relate to a gas volume fraction between 92 and 100 %. The amount of liquid in the gas has a strong impact on the speed of sound and will in turn have a big impact on the critical mass flow rate.

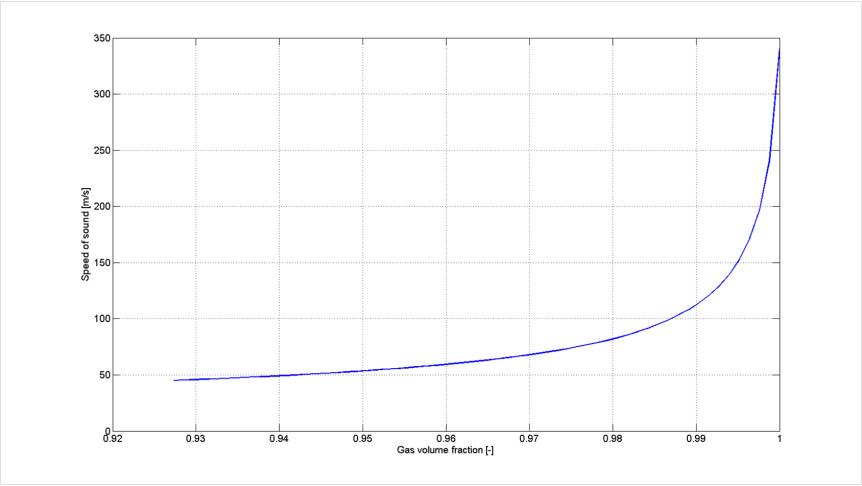

Figure 2.11: Speed of sound compared to gas volume fraction with a liquid mass fraction of 0 and 60%

3 Experimental Studies for Wet Gas Compression

The compositions of the wet gas as well as suction pressure, size and operational speed of the compressor have different impact on the compressor performance, as can be seen when comparing different experiments from different sources [3], [15], [22].

This chapter contains a summary over studied literature and findings others have made. It contains information about different wet gas mixtures such as air/water and hydrocarbon mixtures. It analyses the influence of the suction pressures on the wet gas compressor performance. Many assumptions made in Chapter 4 are based on this chapter.

3.1 Overview Studies

In literature studied, different suction conditions, wet gas mixtures and type of test loops are used.

Fabbrizzi et al. [22] performed tests on a single stage compressor at ambient suction conditions with an air/water mixture in an open loop. Bertoneri et al. [23] presented in 2014 experimental results for an air/water mixture at suction pressures of 10-18.5 bar in a closed loop.

Hydrocarbon tests at 30-70 bar in a closed loop were performed by Brenne et al. [3] and Hundseid et al. [18]. The differences among these tests are summarized in Table 3.1.

Table 3.1: Properties of experimental test runs performed in literature

Author	Wet Gas Mixture	Suction Conditions [bar]	Loop type	Impeller Diameter [m]	Max u_2 [m/s]
Fabbrizzi et al. [22]	Air/water	Atmospheric	Open	0.150	237
Bertoneri et al. [23]	Air/water	10-18.5	Closed	0.370	212
Brenne et al. [3]	Hydrocarbon	30-70	Closed	0.384	216
Hundseid et al. [18]	Hydrocarbon	50-70	Closed	0.384	216

Comparing the compressor used by Fabbrizzi et al. [22], the impeller diameter used by Fabbrizzi et al. is approximately half the size of the ones used by the other authors.

The difference in pressure ratio between a hydrocarbon and air/water mixture can partly be explained by the difference in density ratio for the two different mixtures. The density ratio for an air/water mixture is, in most cases, lower than for a hydrocarbon mixture, which means that the difference in density between the liquid and gas phase is bigger for the air/water mixture. The gravitational force has a higher impact on the liquid phase in the air/water mixture compared to the hydrocarbon mixture. A higher gravitational force on the liquid means lower interaction between the liquid and the gas, which means increased losses.

3.2 Setup

In this chapter, the setup of measurements used in reported experiments and the influence of the injection pattern on the compressor performance are presented.

3.2.1 Measurement Devices and Post-Processing

Today, there is no specific code to perform measurements on a wet gas compression process available. Therefore, different codes, written for dry gas measurements are used to evaluate the wet gas flow in the literature study. Examples on used codes are ASME PTC-10 used by for example Hundseid et al. [18], Brenne et al. [3] and Bertoneri et al. [23]. Bertoneri et al. perform tests according to the standard ASME PTC 19.1.

In a variety of papers studied [3], [23] the suction measurements were performed before mixing of the liquid and gas phase. This could not be performed for the discharge measurements, due to the wetness in the wet

gas mixture. The discharge measurements were performed for the mixture and not for each phase. In different papers [3], [22], the flow of the gas was measured with an orifice plate while the liquid flow was measured with a Coriolis meter. Static pressure measurements were performed through calibrated pressure transducers. To measure the temperature, calibrated thermocouples were used. A schematic diagram of an open wet gas test rig can be seen in Figure 3.1.

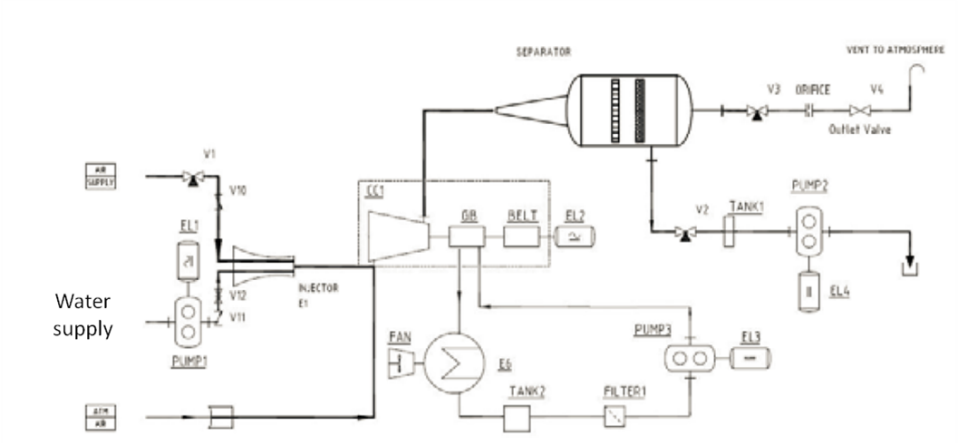

Figure 3.1: Example on a P&ID for an open wet gas test rig. the picture is taken from Fabrizzi et al. [22]

According to Fabbrizzi et al. [22], gas temperature measurements in a wet gas mixture are not accurate, due to the non-equilibrium state of the mixture. Liquid droplets will hit the thermocouple and alter the temperature measurements, due to the high liquid content in the flow. Similar observations are done in different papers. It is not possible to assign temperature measurements taken in the compressor discharge to a specific phase. The temperature has to be evaluated as a temperature of the multiphase mixture, as described by Brenne et al. [3].

3.3 Liquid Injection

The amount of liquid in a wet gas flow has an impact on the performance of the compressor. The flow pattern is important to study, because of wear and tear effects on the compressor. It is not suitable to have a stratified flow through a compressor due to increased wear. The most desirable and due to the high gas velocities and high pressure levels, most probable flow pat-terns are annular dispersed or mist flow.

Brenne et al. [3] have investigated the change in compressor performance if annular dispersed or mist flow is introduced to the suction inlet of the com-

pressor. The two types of flow regimes were introduced through nozzles at a distance from the inlet of the compressor of about three times the internal diameter of the compressor suction inlet. According to the report and what can be seen in Figure 3.2, the difference in performance between a suction flow with a liquid layer on the suction pipe and a dense droplet flow is small. The flow regime present in the compressor inlet is not yet investigated by Brenne et al. A flow introduced as an annular dispersed flow can change to a mist flow, due to high velocities and gas contents. Brenne et al. [3] conclude that the compressor inlet serves as a mixing element and makes the flow pattern inside the compressor wheel relatively independent of which inflow present.

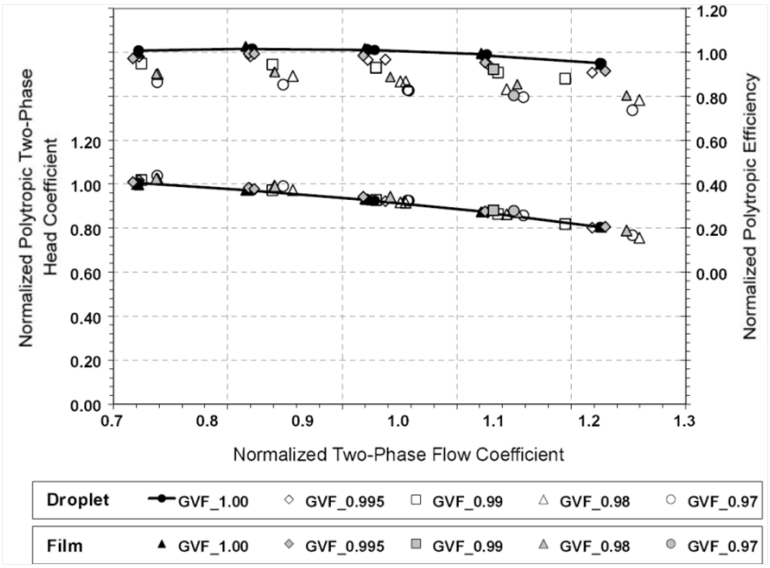

Figure 3.2: Effects on the performance of different liquid injection pattern. Picture is taken from Brenne et al. [3]

Fabbrizzi et al. [22] have investigated the impact of droplet size on a centrifugal single stage compressor when injecting the droplets as a mist flow with and without a suction inlet pipe. When introducing the liquid through a pipe, there was no difference in performance between different droplet sizes. The comparison between wet and dry flow can be seen in Figure 3.3. There are results shown for two tests with two different droplet sizes. The reason to the similar performance for the different droplet sizes is due to liquid formation on the inlet pipe wall. The formation of the layer can be explained as an annular dispersed flow. The droplet size has a bigger impact on the core flow, but when the liquid volume fraction in the different droplet size tests was equal, the difference in droplet size does not matter since the size of the droplets changed before the inlet. The liquid layer formation was dependent on the amount of liquid in the flow and not droplet size when introducing the liquid to the gas flow in a compressor inlet pipe.

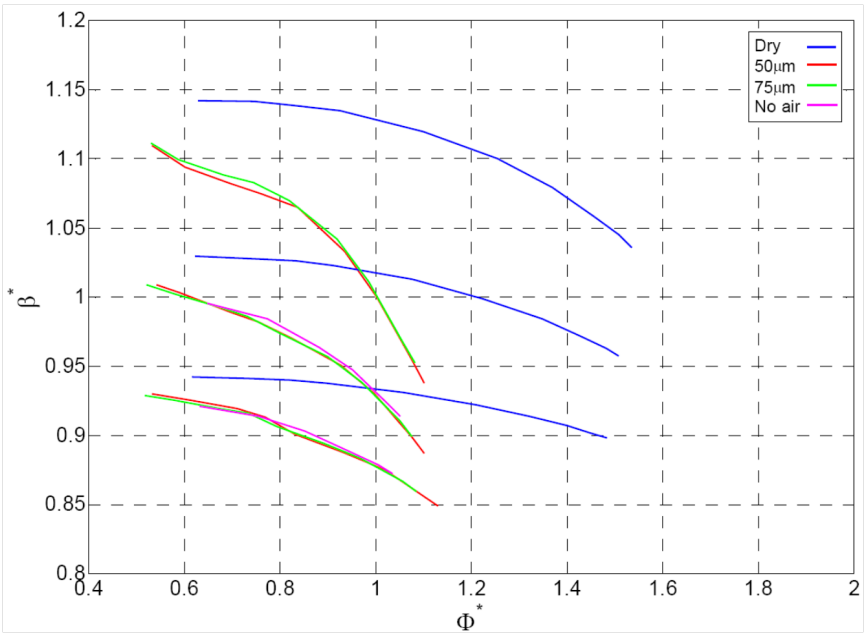

Figure 3.3: Wet compression map for LMF=0.4, with inlet pipe. The blue curve: dry flow, red curve droplet diameters of 50 micrometres, blue curve: droplet diameters of 75 micrometres, pink curve: no air. The picture is taken from Fabrizzi et al. [22]

When introducing the liquid directly into the compressor inlet, the droplet size has an impact on the performance, see Figure 3.4. According to Fabbrizzi et al [22], smaller droplet diameters allow higher pressure ratios. The authors suggest an atomization tool when there is a risk for larger droplet diameters in the flow. A comparison between the two liquid injection patterns was made to investigate the increased wear and tear on the compressor. No evidence for an increased wear and tear was found.

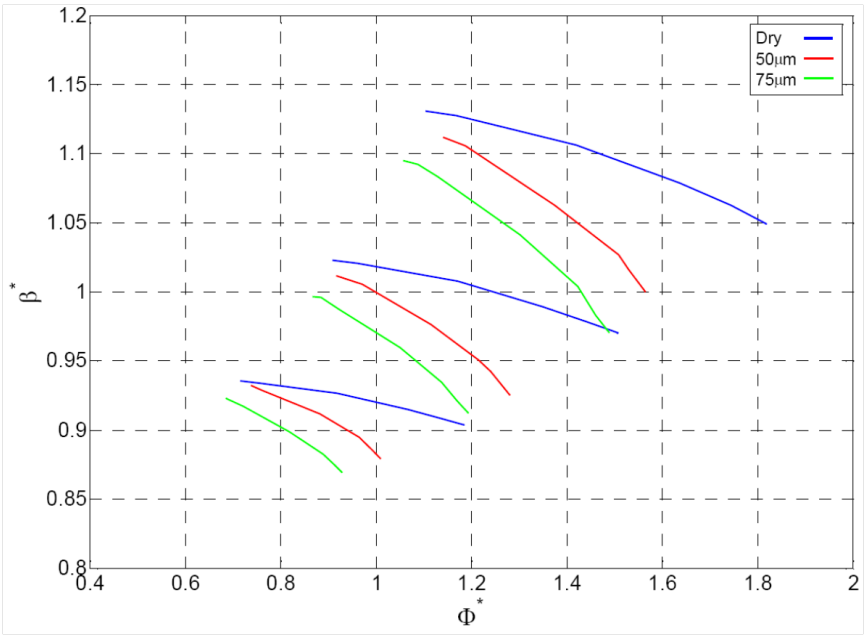

Figure 3.4: Wet compressor map for LMF=0.4, without inlet pipe. The blue curve: dry flow, red curve droplet diameters of 50 micrometres, green curve: droplet diameters of 75 micrometres, taken from Fabrizzi et al. [22]

3.4 Operating Range

To introduce liquid in a gas flow has an impact on the range on the compressor. The impact on the stability and maximum flow are discussed in this section.

3.4.1 Stability Limit

In Figure 3.5, the black line indicates the stability limit of the dry case at highest compressor speed. For these air/water mixtures at atmospheric suction conditions, the stability limit for wet gas flows improves by moving slightly to lower flow coefficients. This observation is not yet confirmed, since it is hard to show if the change in surge is because of the wear and tear effect from liquid droplets, according to Jellum [24].

3.4.2 Maximum Flow

According to Fabbrizzi et al [22], an increased amount of liquid in the flow has an impact on the compressor range, which is indicated by the black arrow in Figure 3.5. The diagram shows 3 different speed lines, where each speed line is measured with 6 different liquid mass fractions. Steeper curves are seen for increased liquid mass fraction, so that maximum flow is significantly reduced. The compressor goes earlier into choke. This is also observed in the test campaigns from Brenne et al. [3] with hydrocarbon mixture and Bertoneri et al. [23] with higher suction pressures compared to Fabbrizzi

et al. The change in range for larger suction pressures and other mixture compositions can be seen in Figure 3.7 and Figure 3.9, from Bertoneri et al. and Brenne et al., respectively. The difference in slopes compared to the dry case is probably due to the inlet distortion and the consequent pressure losses induced by the liquid phase on the gas phase, according to Fabbrizzi et al. [22].

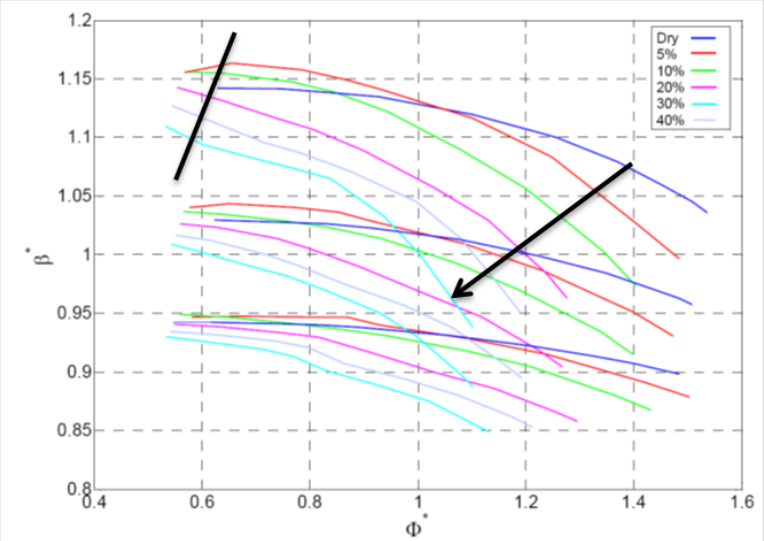

Figure 3.5: Change in range. Compressor pressure ratio versus flow rate for three different motor speeds, n=20′000, 25′000, 30′000 rpm. The mixture is air/water at ambient conditions as inlet conditions and the plot axes are normalized. The picture is taken from Fabrizzi et al. [22]

Another explanation to the decrease in range is liquid blockage of the impeller, which means that the effective stage flow channel is smaller, see illustration in Figure 3.6. The liquid layer flows along the walls and lead to an earlier choke of the compressor. According to Hetsroni [14], the size of the liquid void fraction ε_L is an approximation of the blockage area. A liquid volume fraction of 6 % may correspond to a much higher blockage than 6 %, if the liquid propagates at lower speeds than the gas. Especially for low density ratios δ the liquid propagates at lower speeds.

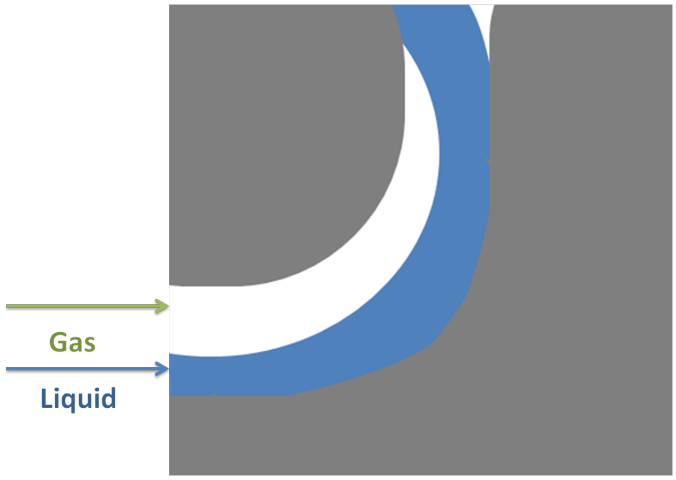

Figure 3.6: Illustration of the liquid blockage in a radial compressor impeller

3.5 Pressure Ratio

It is seen that the gas composition has an impact on the change in pressure ratio for a wet gas flow compared to dry gas flow. Therefore, this section is divided into two sections presenting the wet pressure ratio according to gas mixture.

3.5.1 Air/Water Mixture

According to Fabbrizzi et al [22] and Bertoneri et al [23], liquids in general, have a negative influence on the compressor pressure ratio, as illustrated in Figure 3.5 and Figure 3.7, which show results for two different test periods and different suction conditions.

For atmospheric suction conditions, Fabbrizzi et al [22] have seen that by adding liquid to the gas flow, the pressure ratio changes. For cases with a liquid mass fraction below 10 % at low flow rate coefficients, the pressure ratio is higher compared to the dry compression. The result is more or less similar independent on rotational speed level for the test. One explanation is that the gain in pressure results from the increased flow density of the wet gas compared to the dry gas. Another explanation is, according to Fabbrizzi et al. [22] and Bertoneri et al. [23], that the intercooling by the liquid phase has a positive impact on the pressure ratio, due to decreased suction temperature, when the liquid evaporates. The decrease in suction temperature leads to a lower volume flow, which makes it possible to compress a higher volume flow rate. This process leads to lower discharge temperature and higher discharge pressure, which means a higher pressure ratio compared to the dry case.

For increasing water mass fractions, the air becomes saturated and the additional water will flow as liquid phase. This leads to higher losses as dis-

cussed in Chapter 2.3.4. When these losses exceed, the positive impact from the change in density, the pressure ratio will decrease and be lower than for the dry case.

For higher suction pressures, the effects of a liquid phase are similar to low suction pressures. In the region close to surge, it is possible to receive a pressure gain compared to the dry gas case. A reduced range is seen, similar to lower suction pressure.

For a higher pressure, a pressure gain at lower flow coefficients of the whole stage is seen for liquid mass fractions larger than 30 % for an air/water mixture. This can be seen in Figure 3.7.

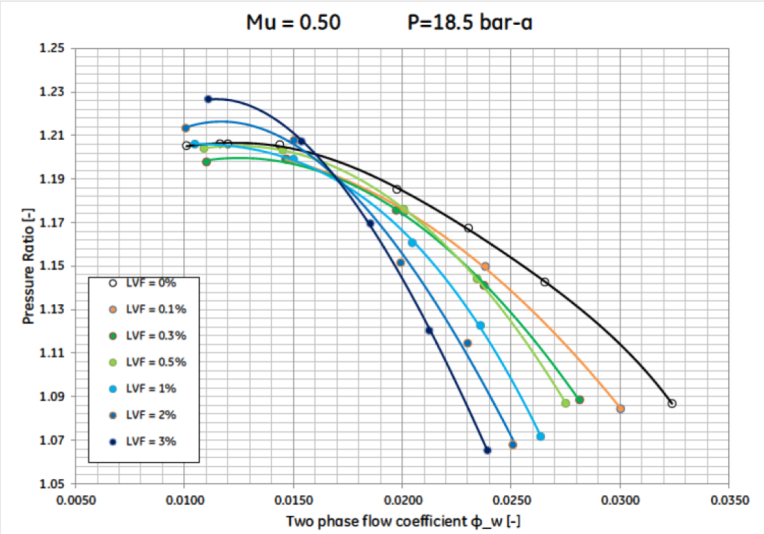

Figure 3.7: Flange to flange pressure ratio at a suction pressure of 18.5 bar for LVF=0.1%, 0.3%, 0.5%, 1%, 2%, 3%, which equals LMF = 4%, 12%, 19%, 31%, 58%, 70%. The diagram is from Bertoneri et a. [23]

Bertoneri et al. [23] measured the pressure increase over the impeller of the compressor, see Figure 3.8. The pressure ratio constantly increases with increasing liquid mass fraction. According to the authors, the difference in pressure gain for impeller measurement and flange to flange measurement is because of the increased losses over the static parts, such as the diffuser in the stage.

When a higher suction pressure is used, a larger gain in pressure ratio compared to the case with atmospheric suction conditions is obtained. One interesting observation when comparing the two cases to each other is that Bertoneri et al. [23] receive a higher pressure ratio for a higher liquid volume fraction, where Fabbrizzi et al. [22] already received a decrease compared to the dry gas run. According to Bertoneri et al [23], the larger pressure

ratio for larger liquid volume fractions is due to a higher fluid density, the cooling effect of the liquid evaporation and the speed of sound variation in a two-phase flow. For higher flow coefficients, the increase in losses are higher than the positive effects from, for example, the change in density and the pressure ratio is lower than the dry reference run.

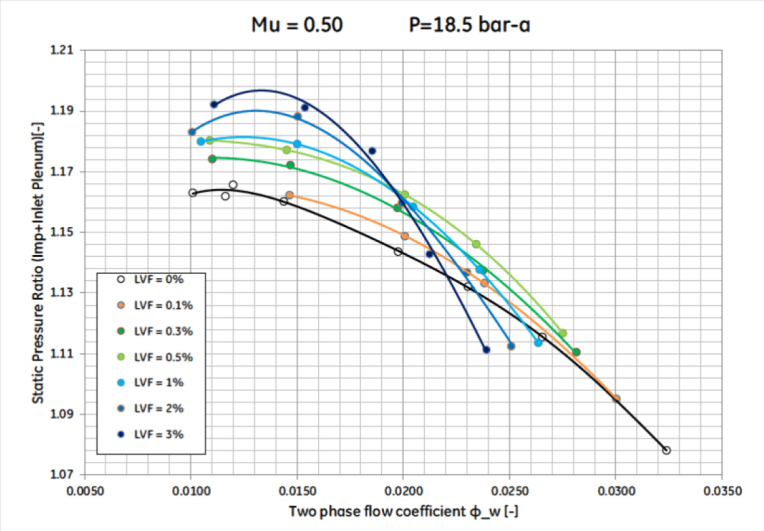

Figure 3.8: Impeller static pressure ratio compared to the flow coefficient for LVF= LVF=0.1%, 0.3%, 0.5%, 1%, 2%, 3%, which equals LMF = 4%, 12%, 19%, 31%, 58%, 70%. The diagram is from Bertoneri et a. [23]

3.5.2 Hydrocarbon Gases

The experiments with hydrocarbon gases behave different compared to air/water experiments. This can partly be explained by the higher density ratio, as discussed in Chapter 3.1 The air/water mixture has a lower density ratio than the hydrocarbon mixture and thus a lower gas-liquid interaction. The higher interaction may have a positive effect promoting pressure rise, but it also increases losses such that the sum of these competing effects has to be analysed.

According to Brenne et al. [3], the presence of wet gas has an increasing effect on the pressure ratio, as shown in Figure 3.9. The reason for why the overall higher pressure ratio over the complete stage can be explained by the mentioned density change and coherent intercooling effects.

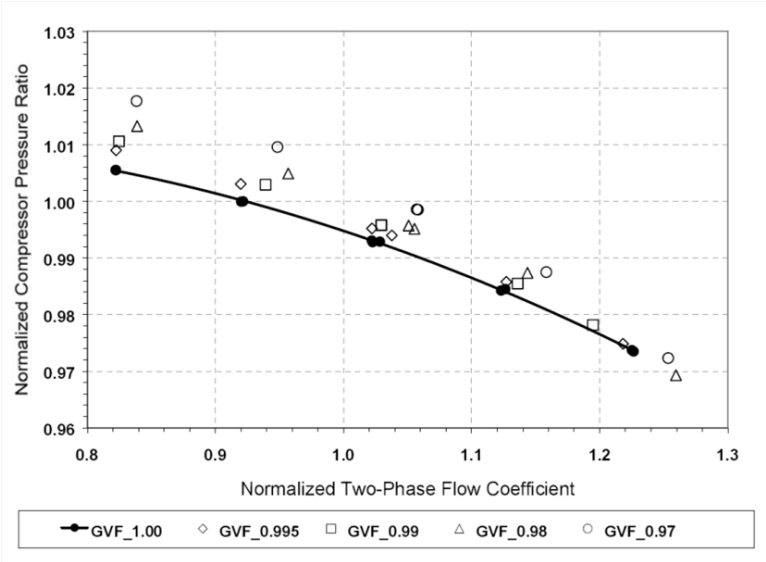

Figure 3.9: Normalized compressor pressure ratio as a function of Gas Volume Fraction for natural gas at a suction pressure of 70 bar, GVF = 0.995, 0.99, 0.98, 0.97 correspond to LMF=5.5%, 10.5%, 19%, 26%, respectively. The diagram is from Brenne et al [3]

Hundseid et al. [18] show further results from the same measurement campaign at a suction pressure of 50-70 bar which is shown in Figure 3.10. According to Hundseid et al, the better pressure ratio compared to the dry case is a sign on limited evaporation in the compression process.

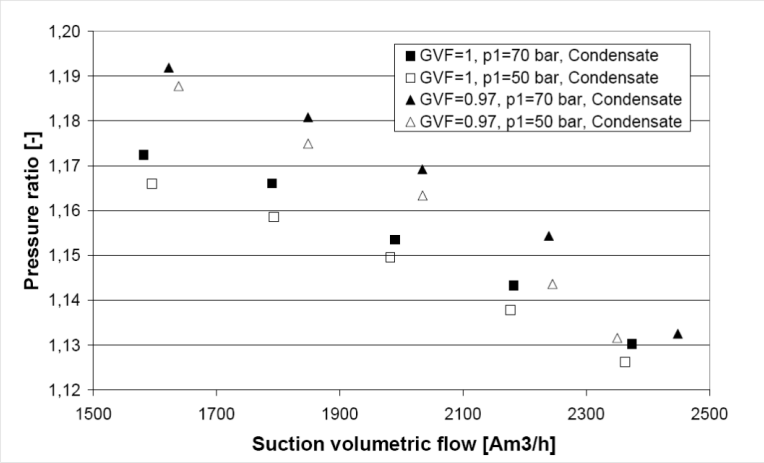

Figure 3.10: Pressure ratio for natural gas as a function of suction volume flow rate at suction pressures of 50 and 70 bar. The diagram is taken from Hundseid et al. [18]

3.6 Power Consumption

The power consumption of a compressor with wet gas is higher when comparing it to dry compression. According to Bertoneri et al. [17], the increase in internal losses and the greater mean density requires an increased required power, see Figure 3.11.

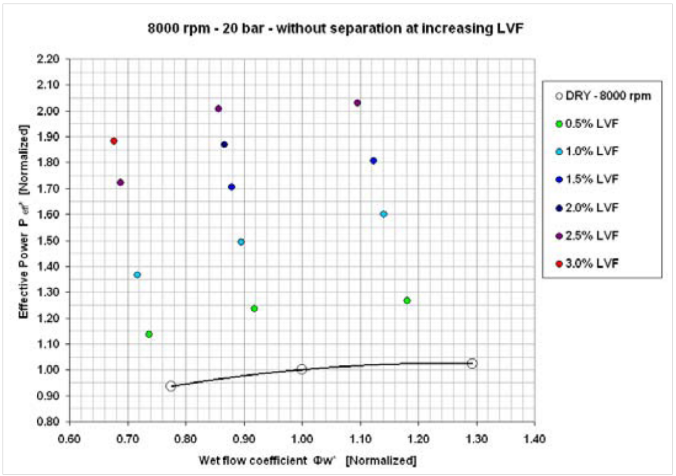

Figure 3.11: Normalized effective power compared to wet flow coefficient for LVF=0.1%, 0.3%, 0.5%, 1%, 2%, 3%, which equals LMF = 5%, 13%, 20%, 33%, 50%, 60%. The diagram is taken from Bertoneri et al. [17]

3.6.1 Power Evaluation of the Compressor Performance

To become trustworthy measurement for the different phases in the compressor discharge is difficult, due to the two-phase mixture. Other solutions to determine the performance of a compressor are reported. An often used parameter is the comparison between dry and wet shaft power

$$\frac{P_{wet}}{P_{dry}} \tag{3.1}$$

This ratio will in many cases be higher than 1, since the process requires an increase in work due to the liquid phase in the flow. It can be seen in Figure 3.11, the shaft power increases close to linearly for increasing liquid mass fraction.

3.7 Efficiency

In this chapter, different methods to calculate the efficiency are reported. The liquid phase causes problems when measuring the discharge temperatures, so alternative evaluation parameters need to be used, such as shaft power for wet gas compression compared to a dry gas reference compression.

3.7.1 Polytropic Efficiency

The formula of how to calculate the polytropic efficiency is described in Chapter 2.1. To calculate the polytropic efficiency the suction and the discharge conditions, such as pressure and volume flow, need to be known. As written before, it is not possible to receive trustworthy measurements of the temperature and thus the volume flow in the discharge of the compressor, due to the liquid phase. When not knowing the discharge conditions, the polytropic efficiency cannot be calculated with trustworthy results. See a comparison between a dry case and wet case for a two stage compressor compressing an air/water mixture in Figure 3.12.

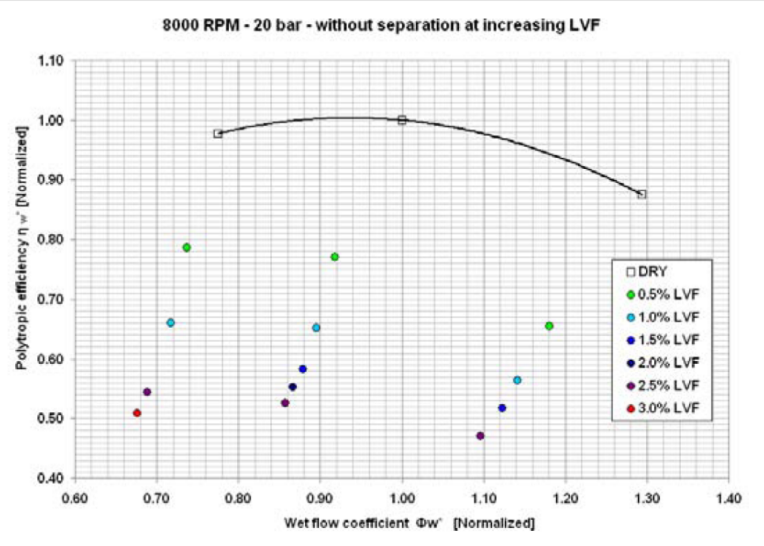

Figure 3.12: Normalized polytropic efficiency compared to normalized wet flow coefficient. The diagram is taken from Bertoneri et al. [17]

3.7.2 Work Coefficient

A common used expression to use for evaluation of the wet gas process of a compressor is the work coefficient. The work coefficient is calculated from the measured shaft power and the mass flow rate of the wet gas flow. The work coefficient is calculated and shown in Figure 3.13. According to Bertoneri et al. [17], the work coefficient does not change with the liquid mass fraction, if the work coefficient is computed from the ratio of shaft power over total mass flow rate.

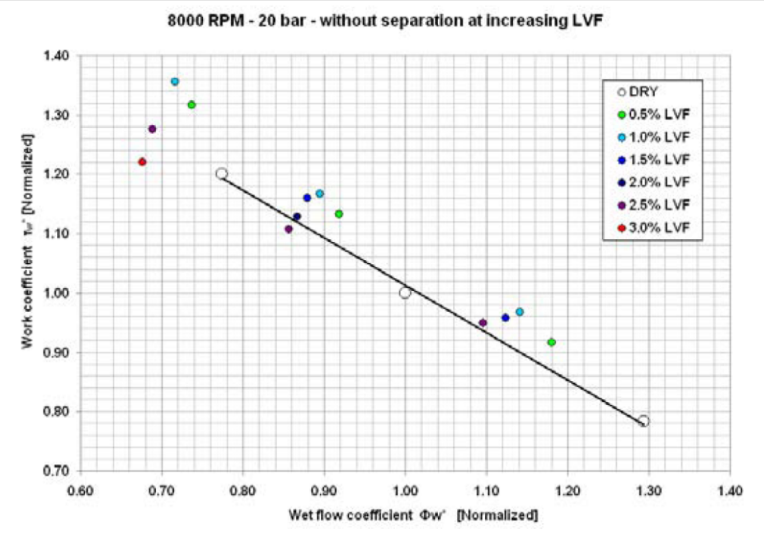

Figure 3.13: Normalized work coefficient compared to normalized wet flow coefficient. The diagram is taken from Bertoneri et al. [17]

3.8 Vibrations

According to a variety of sources [22], [23], the presence of a liquid phase in the compression does not increase the lateral, axial and torsional vibrations significantly. Brenne et al. [3] have seen that when the liquid is introduced as droplets into the gas flow, it does not introduce further vibrations to the compressor, see a comparison in Figure 3.14. The upper diagram shows vibrations in the process for a wet run with a gas volume fraction of 97 %, which corresponds to about 74 % gas mass fraction, at a rotational speed of 9651 rpm. The lower diagram is for the corresponding dry case. When the liquid is distributed in a uniform manner, it does not seem to be a significant source of rotor excitation or unbalance to disturb the rotor dynamic behaviour.

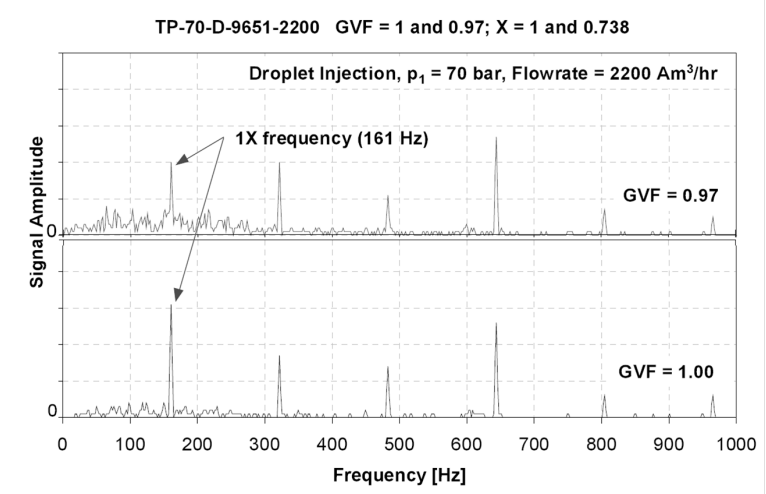

Figure 3.14: Comparison of vibration between a wet (above) and a dry (below) run [3]

3.9 Erosion and Corrosion

The presence of erosion and corrosion is investigated by a variety of sources [3], [22], [23], [25]. Bertoneri et al. [23] performed erosion tests with soft paintings. The authors conclude that the most exposed areas for erosion is at the

- impeller inlet hub and leading edge
- impeller trailing edge on pressure side

During the short period of four weeks, no signs on erosion could be seen. Not yet investigated is the effect for longer terms. Madsen et al. [25] have investigated the presence of erosion from water liquid droplets on a gas turbine at a liquid mass fraction of 0.5-1.0 %. At this low liquid mass fraction, no signs on erosion could be seen.

In the investigation performed by Brenne et al. [3], no evidence of erosion could be found. However, the inner of the compressor was cleaned by the injected liquid.

3.10 Summary

To run a compressor under wet gas conditions adds complexity compared to dry gas operation. The liquid phase in the process makes it difficult to receive trustworthy measurements, especially for temperature measurements. For the suction flow, separate measurements for each phase may be received, but in the discharge of the compressor, it is not possible to receive the temperature of each phase. Therefore, the efficiency evaluation of the process is

more complicated than for a dry case. When evaluating a wet gas compression process, the shaft power is usually compared to a dry reference run.

Depending on which wet gas mixture, number of stages and suction conditions used, the pressure ratio will be higher or lower compared to a dry compression. For a hydrocarbon mixture at elevated suction pressure, where the differences in behaviour between liquid and gas phase are less than for an air/water mixture, a higher pressure ratio compared to a dry reference run is received. For an atmospheric air/water mixture the pressure ratio is only higher for cases where the liquid mass fraction is below 10 %.

The required power in a wet gas compression process increases, due to additional mass of the liquid. The liquid phase introduces an increase in losses, such as acceleration losses such that the additional power does not necessarily lead to higher pressure ratios.

An increase in vibrations has not been seen when having a uniform distribution of liquid drop-lets in the compression process.

Erosion does not seem to be a problem in the studied literature, given short term investigations. However, the liquid seems to have a cleaning effect on the inner parts of the wet gas compressor.

4

Wet Gas Analysis and Modelling

An investigation of suction flow regimes is done and the result is plotted in two different Baker diagrams. A dry gas model and a model for wet gas are reported.

4.1 Analysis of Different Wet Gas Flow Measurement according to Flow Map

In Chapter 2.3.3, wet gas flow regimes were discussed. An investigation of compressor suction flow regimes for different suction pressures, wet gas mixtures and rotational speeds is performed. The results are based on data found in literature for different suction pressure levels and rotational speeds and wet gas mixtures. The results are plotted in the flow diagrams developed by Shell DEP [21] and Scott et al. [20], see Figure 4.1 and Figure 4.2, respectively.

In the diagram from Shell [21], the results for pressure level at 1 bar indicate on a wavy stratified flow. For a wavy stratified flow the phases flow separate from each other. The liquid phase flows on the bottom of the pipe, due to gravity. This means a bad mixing of the two-phase flow. This agrees with the observations for low suction pressures at atmospheric conditions. A rapid separation of gas and liquid was observed, which required spraying the liquid close to the compressor suction in order to avoid separation.

For higher pressure levels, the diagram indicates flows closer to or in the annular dispersed region. This means more homogenous multiphase flow. For high pressures, the density ratio of gas over liquid increases, indicating that the interaction between the phases are stronger, leading to better mixing.

Also in the diagram of Scott from 1963 [20], the results for 1 bar are found in the wavy stratified region. For increased pressure ratio, the flow regime changes to annular dispersed flow. The results for low pressures are shifted to the left and found outside the diagram area. This diagram is probably

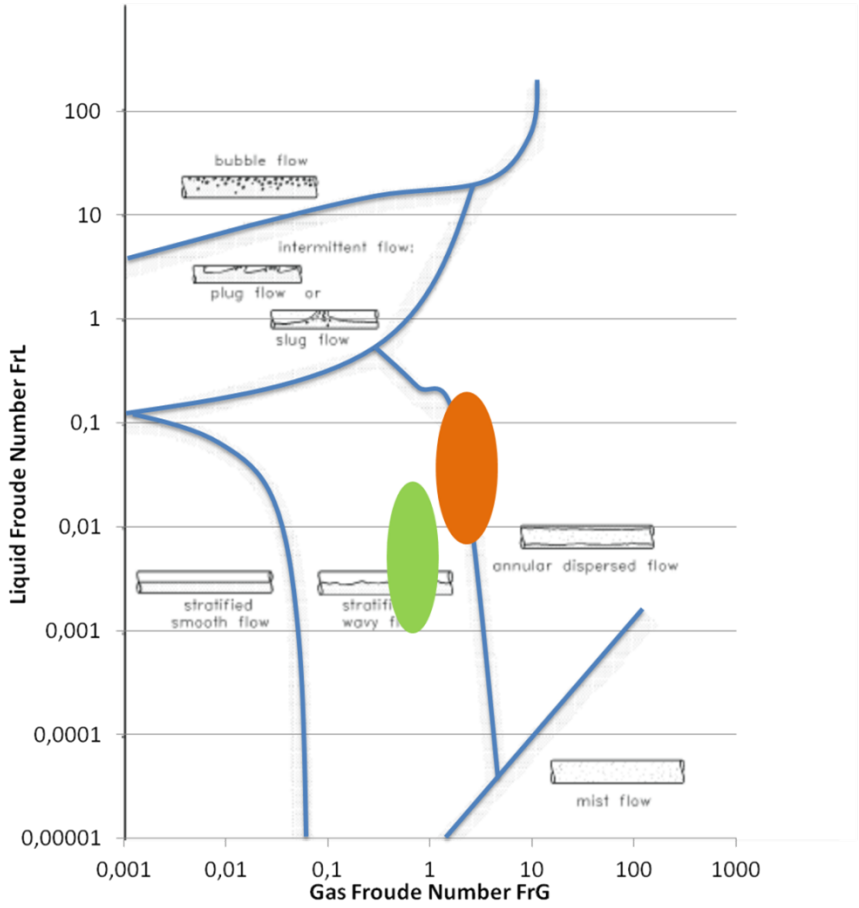

Figure 4.1: Result of the investigation of flow regime in the suction pipe of the compressor for different suction pressures and rotational speeds. The flow diagram is produced by Shell [21]

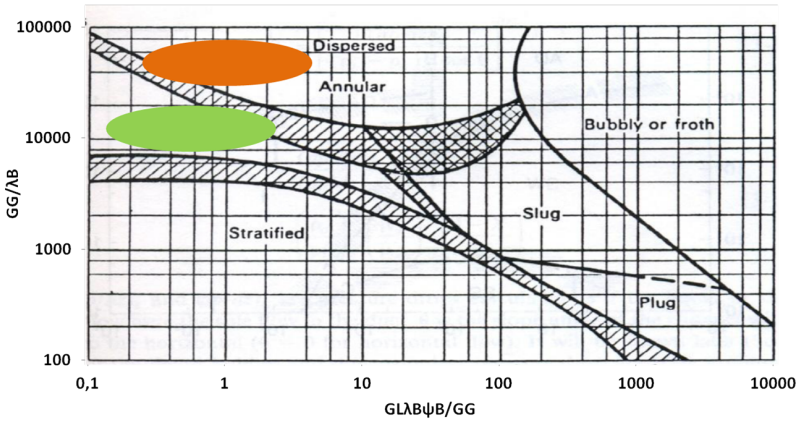

Figure 4.2: Result of the investigation of flow regime in the suction pipe of the compressor for different suction pressures and rotational speeds. The flow diagram is produced by Scott [20]

not designed for such low liquid fractions which are found in the studied wet gas flows.

The diagrams show slightly different results, probably due to the different reference mixture. However, the results shown in the diagrams are indications on which flow regime present for a two-phase flow.

4.2 Model For Dry Gas Calculations

As a first step to create a compressor model for wet gas compression, a model for dry gas compression is created. In this chapter, a model for dry gas is presented. Uncertainties are discussed.

For the dry gas model, measurement data is used for validation. For the model, suction pressure, temperature and mass flow rate are used and also the cooling gas mass flow rate. Measured and calculated values are compared and presented as the *relative error* ϵ

$$\epsilon = \frac{x_m - x_c}{x_m} \tag{4.1a}$$

The relative error is based on the measured value. A negative relative error means that the calculated value is higher than the measured value.

4.2.1 Uncertainties in the Model

When creating a wet gas model, the gas composition is important to know. To create a gas matrix for a gas composition different to the original one gives slightly different results in the comparison.

There are different implementations of equations of states available to create a gas matrix. Depending on which equation of state used, a different result of the performance of the compressor is received, as written by Hundseid et al. [26]. For a comparison between two different calculations, it is important to use the same implementation of the equation of state.

4.2.2 Model

The dry gas model is developed for a radial compressor with a variable number of stages. For the dry gas model, the calculation is based on the PTC10-code.

The compressor model process is based on given suction conditions, such as suction pressure, temperature and mass flow rate. If there are extractions in the process, they are added. Thereafter, the iteration process over the number of stages starts. For each stage, polytropic efficiency, pressure coefficient and power coefficient are calculated. These values give the discharge enthalpy and entropy. The pressure and temperature are calculated from a gas matrix based on the chosen implementation of the equation of state.

4.2.3 Symbols

To be able to distinguish between measured and calculated values, different symbols are used. The symbols are shown in Figure 4.3. For measured values a down pointing triangle is used and for calculated values a cross.

Figure 4.3: Symbols used in plots for the dry model. Triangle indicates measurements and cross indicates calculations

4.2.4 Results

The computed values for the dry compressor model show acceptable results. Compared to measured values, the calculated compressor is in some cases slightly bigger than the measured compressor. Since the computations do not show clear signs on a systematic error the model is considered to pass. The mean relative error is less than 5 %.

The operating points for low rotational speeds, the rear stages are closer to choke than for operating points at high rotational speeds. The rear stages operate at higher volume flows than designed for thus closer to choke than the front stages.

The calculated and the measured pressure ratio and the shaft power for a suction pressure and a rotational speed can be seen in Figure 4.4.

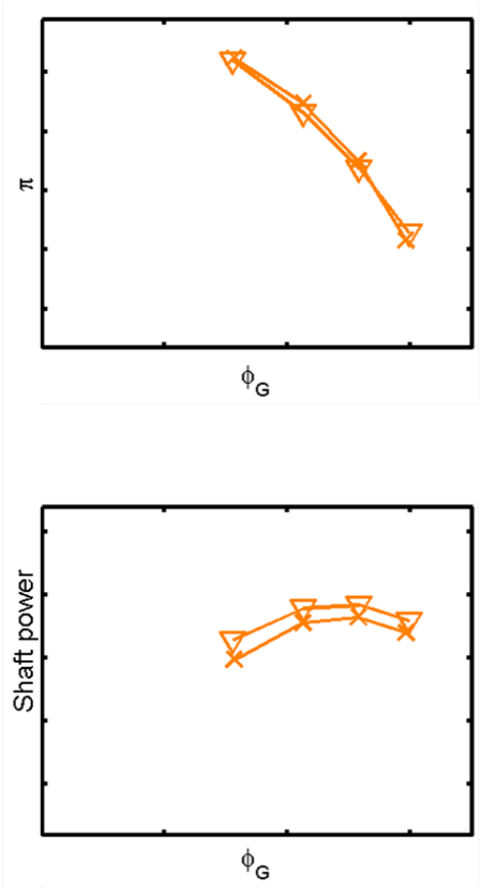

Figure 4.4: Illustration of the pressure ratio (above) and the shaft power (below) for a dry gas computation

4.3 Wet Gas Operation

When introducing liquids to the testing, different phenomena occur which have different impact on the performance of the compressor. In this chapter, from the literature found effects on the performance of a wet gas flow are presented.

The proposed model in this report is based on wet gas flow in pipes. In the beginning of this report, it was discussed to generate a complete new model for wet gas compression in a radial compressor. After the literature study, it was seen that there are many unknown effects introduced by the liquid phase in the flow. A decision was made to base the model on a well-investigated area such as multiphase flows in pipes, but to introduce also observed effects from the literature studied.

In Chapter 3, it was observed that the pressure ratio increases for a hydrocarbon mixture at pressure levels above 30 bar, [3]. For an air/water mixture, the higher pressure ratio compared to a dry reference case, was seen at low flow coefficients only. At atmospheric conditions, the liquid mass fraction must also be below 10 %, see Figure 3.5. It was seen that for both hydrocarbon mixtures as well as for air/water mixtures, the maximum flow was decreased for increased liquid mass fractions and the pressure ratio curve was steeper.

From these observations, it is possible to say that the impeller tip speed, the suction pressure and the amount of liquid in the wet gas flow have an impact on the discharge pressure. The pressure ratio is a function of the rotational speed, the suction pressure level and the liquid mass fraction

$$\pi = f(N, p_{in}, LMF) \tag{4.2a}$$

In Figure 3.11, the increase in shaft power can be seen. The power increases linearly with the increase in liquid mass fraction. This means that the power is a function of the liquid mass fraction

$$P_{wet} = f(LMF) \tag{4.3a}$$

The operating range decreases for increased liquid mass fraction.

4.4 Model for Wet Gas Calculations

The compressor model for a wet gas compression is based on the dry compressor model but with modifications. In this chapter, the model is presented and corrections due to the wet gas are shown.

4.4.1 Uncertainties and Limitations in the Model

The model is based on the dry gas model as described in Chapter 4.2. This means that the uncertainties described in Chapter 4.2 are valid for the wet

gas model.

4.4.2 Model

The model consists of two correction steps, see illustration in Figure 4.5. The corrections are mainly focused on correction of the stage characteristics, but the power is corrected by the increase in mass flow due to the liquid phase. The first step focuses mainly on the seen earlier blockage of the compressor for increased liquid volume fraction in the flow and a new operating point is calculated. Thereafter is the stage characteristic corrected with the seen effects described in Chapter 4.3.

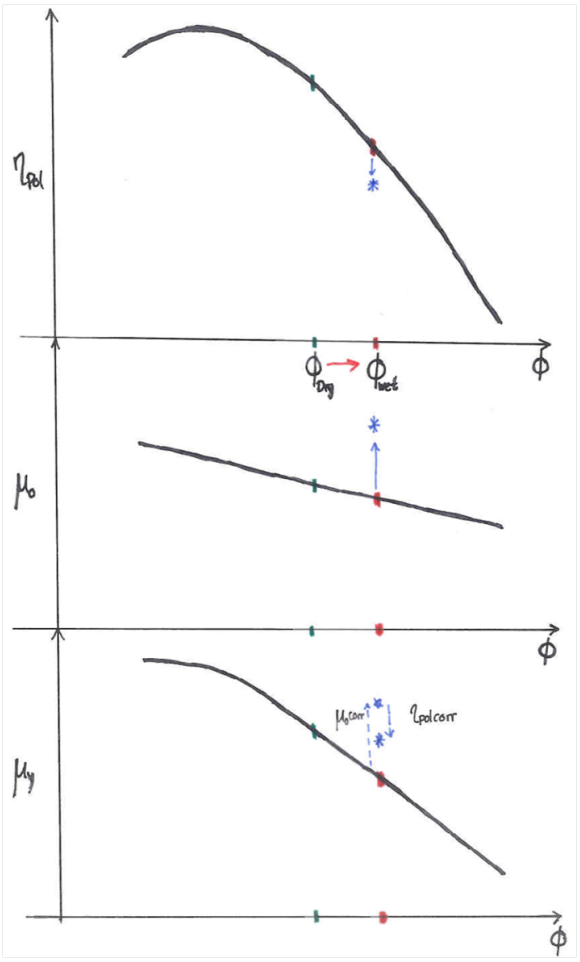

Figure 4.5: Illustration of the adjustment of one point in the compressor stage characteristics for a wet case. Green colour indicates dry values; red is adjustment of the flow coefficient and blue is the individual adjustment of each parameter.

There are two different correction versions proposed. Each version gives slightly different results.

Version 1 corrects the pressure coefficient with a function of the liquid mass fraction, the rotational speed and the density ratio. The flow coefficient is adjusted by a function containing the gas volume fraction.

Version 2 is built upon the homogenous model of multi-phase flow, as described in Chapter 2.3.4. The power coefficient and the polytropic efficiency are adjusted by a function of the gas mass fraction, the density ratio and the rotational speed. The flow coefficient is adjusted by a function of the gas volume fraction.

First, the correction process is described. The correction factors for the two versions are discussed more in detail later.

In the first step, the observation concerning the earlier choke of the compressor for increasing liquid content in the flow is taken into account. This means that the compressor can be seen as a smaller machine and the operating point must be moved closer to the choke limit in the characteristics. This is done through a correction of the gas flow coefficient. From the new flow coefficient, a new operating point is calculated for the pressure coefficient and power coefficient.

$$\phi_w = CorrPar1 \cdot \phi_G \tag{4.4a}$$

The stage characteristics are calculated

$$\mu_{y_{corr1}} = \mu_y(\phi_w) \tag{4.5a}$$
$$\mu_{0_{corr1}} = \mu_0(\phi_w) \tag{4.5b}$$

In the second step, the increase or decrease in the characteristic values is taken into account. As written in Chapter 4.3, the pressure ratio and the power increase for increased pressure levels and rotational speeds.

In version 1, the pressure coefficient is corrected by a correction parameter

$$\mu_{y_w} = CorrPar2 \cdot \mu_{y_{corr1}} \tag{4.6a}$$
$$\mu_{0_w} = \mu_{0_{corr1}} \tag{4.6b}$$
$$\eta_{pol_w} = \frac{\mu_{y_w}}{\mu_{0_w}} \tag{4.6c}$$

By doing these corrections, the discharge pressure and the polytropic efficiency are adjusted. As reported earlier, the additional power is more or less constant over the pressure levels but increases with increased liquid mass fraction in the flow, see Chapter 4.3. The modified power calculation is

$$P = (\dot{m}_G + \dot{m}_L) \cdot \Delta h_{0_G} \tag{4.7a}$$

In version 2, the first step is equal to version 1. The flow coefficient is adjusted by a correction parameter. In the second step, the pressure coefficient and the polytropic efficiency are adjusted to consider the increase in discharge pressure, which is described in Chapter 4.3, and the more losses due to the introduced roughness from the liquid phase. The power coefficient is calculated from these changes.

$$\mu_{y_w} = CorrPar2 \cdot \mu_{y_{corr1}} \tag{4.8a}$$

$$\eta_{pol_w} = 1 - (1 - \eta_{pol_G}) \cdot CorrPar2 \tag{4.8b}$$

$$\mu_{0_w} = \eta_{pol_w} \cdot \mu_{y_w} \tag{4.8c}$$

The shaft power for version 2 is calculated for the liquid phase and the gas phase separately. It is assumed that the heating of the liquid through the compression process is negligible. The power required to compress the liquid phase is the pump work

$$P_L = \dot{V}_L \cdot \Delta p \tag{4.9a}$$

The remaining increase in shaft power is put on the gas phase and is affected by the adjustments described in equation (4.8). The total shaft power for the computed process is the sum of the required power to compress the gas respective the liquid phase

$$P_w = P_G + P_L = \sum_{stages} (\dot{m}_G \cdot \Delta h + \dot{V}_L \cdot \Delta p) \tag{4.10a}$$

The assumption of an adiabatic liquid compression process might lead to a too small computed shaft power. To receive a higher shaft power, the heating work of the liquid phase can be added to the model and version 2. The shaft power would be

$$P_w = P_{G_{compression}} + P_{L_{pump}} + P_{L_{Heating}} \tag{4.11a}$$

Adjustments on the polytropic efficiency and the pressure coefficient have a direct effect on the discharge conditions.

4.4.3 Correction Factors

The correction parameters for the two correction versions are defined in this chapter.

Version 1

Version 1 is based on pressure losses for a two-phase flow in a pipe. These are described in Chapter 2.3.4.

The adjustment for earlier choke is done for the first correction parameter. The first correction parameter is based on the homogenous model for a two-phase flow. It is assumed that the effect of the different phase velocities are

negligible and that it is the amount of liquid in the two-phase flow which has the biggest effect on when choke of the compressor appears. The first correction parameter is based on the gas volume fraction

$$CorrPar1 = \frac{1}{GVF} \tag{4.12a}$$

This correction parameter moves the flow coefficient closer to choke, which means that there will be earlier choke when compressing a wet gas flow. The more liquid it is in the flow, the bigger the correction parameter is. When there is a dry gas flow, the correction parameter will be 1, which means that the gas losses are considered.

The second correction parameter for the power coefficient is based on the multiplier Φ_G, which is introduced in chapter 2.3.4.

$$\Phi_G = 1 + C \cdot X + X^2 \tag{4.13a}$$

For a two-phase flow with a maximum liquid volume fraction of 5 %, the third term on the right hand side is small and can be neglected.

The constant C is described to consider type of flow path. For a compression process the conditions are different compared to the flow in a pipe. However, the constant is used to adjust the model to fit the conditions for a specific case. In this report, it is used to adjust the flow to a wet gas compression process.

As described in Chapter 4.3, the pressure change is dependent on the liquid mass fraction, the density ratio and the velocity of the compressor. The Lockhart-Martinelli parameter handles the density ratio and the fraction of liquid in the flow. The constant C is modified to handle the effect from the impeller tip speed of the compressor

$$C = (\frac{u_2}{u_{2_{ref}}})^{0.35} \tag{4.14a}$$

The exponent in equation (4.14) was chosen to fit seen conditions for a wet gas compression process. The third term in equation (2.52) is negligible.

The multiplier for a two-phase flow through a compressor is

$$CorrPar2 = 1 + (\frac{1 - GMF}{GMF})^{0.9} \cdot (\frac{\rho_G}{\rho_L})^{0.5} \cdot (\frac{\mu_L}{\mu_G})^{0.1} \cdot (\frac{u_2}{u_{2_{ref}}})^{0.35} \tag{4.15a}$$

With $u_{2_{ref}}$ equal the lowest speed.

For a wet gas flow, the pressure losses due to the gas phase are included and also the losses due to interaction between the liquid and the gas phase.

Version 2

Version 2 is based on the homogeny model, where the two phases in the wet gas flow are assumed to have equal velocity. In this case, the assumption is made that the difference in the velocity does not have a big effect on the performance. The correction parameters for version 2 are based on the volume and mass fraction.

Correction parameter 1 for version 2 is equal to the correction parameter described for version 1.

$$CorrPar1 = \frac{1}{GVF} \tag{4.16a}$$

The correction parameters for the pressure coefficient and the polytropic efficiency are based on a philosophy, where the liquid mass fraction has the biggest impact on the modelling of the compressor. The correction parameters are therefore based on the gas mass fraction.

$$CorrPar2 = \frac{1}{GMF} \tag{4.17a}$$

$$\tag{4.17b}$$

For a wet gas flow with increasing liquid mass fraction, the three correction parameters will increase. When there is a dry gas flow, no correction will be done and the compressor process is computed as for the dry gas process.

4.4.4 Results for Different Size of the Liquid Mass Fraction

The values for the correction parameters for the different versions vary between 1.0 and 1.3 for correction parameter 1 *CorrPar1* and correction parameter 2 *CorrPar2* for both version 1 and 2.

A change in flow coefficient and power coefficient can be seen for the corrections in version 1. An illustration can be seen of the change in power coefficient for version 1 in Figure 4.6. The corrections for version 1 have an effect on the change in flow coefficient and on the power coefficient. For increased liquid mass fraction, the correction on the flow coefficient increases and so do also the power coefficient. This will have an effect on the polytropic efficiency, which will be higher compared to the dry case. Stars indicate the value of the gas flow coefficient and the triangles the second correction values.

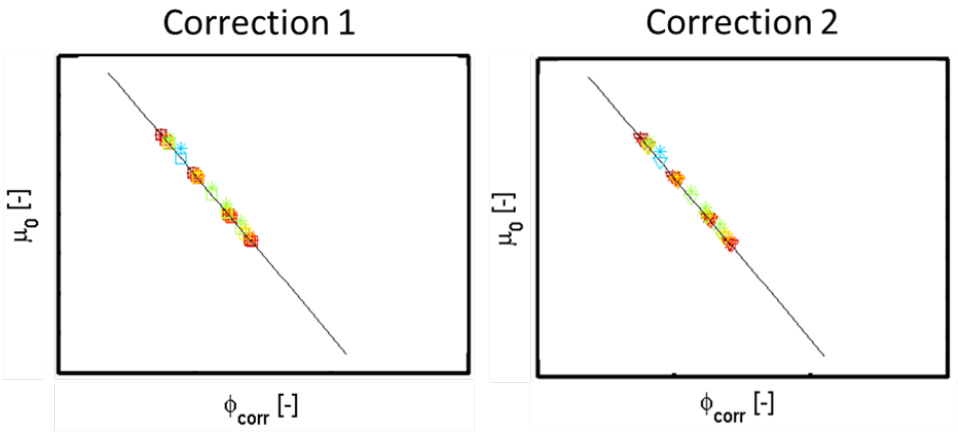

Figure 4.6: Change in power coefficient for version 1, correction 1 (left) and correction 2(right)

For version 2, the increase in pressure and increased losses, which means lower polytropic efficiency, are simulated with corrections on the pressure coefficient and polytropic efficiency. The effect on the power coefficient of the two correction steps can be seen in Figure 4.7. For correction 1, the flow coefficient is shifted closer to choke. Correction 2 gives higher pressure coefficient and lower polytropic efficiency, which gives a higher power coefficient.

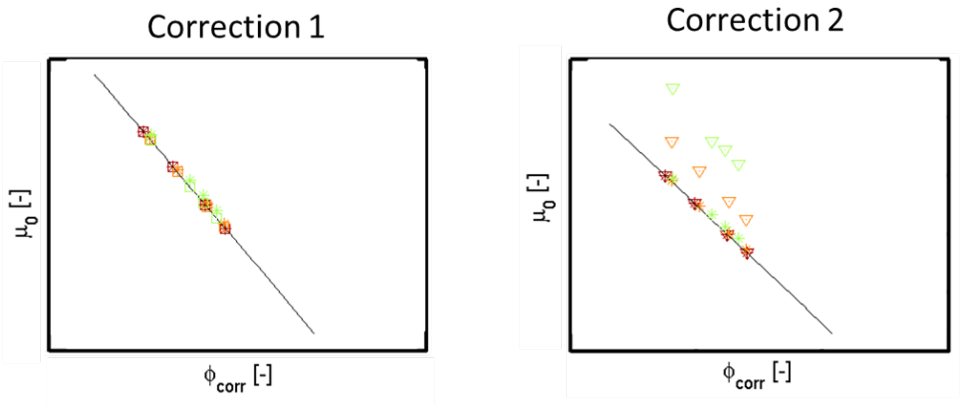

Figure 4.7: Change in power coefficient for version 2, correction 1 (left) and correction 2(right)

The results for the different correction versions are shown below. The diagrams are shown for one suction pressure level and rotational speed and for different liquid mass fractions.

Version 1

The pressure ratio for version 1 can be seen in Figure 4.8. The decrease

in maximum flow is received. The steepness in the curves is not received for larger flow coefficients.

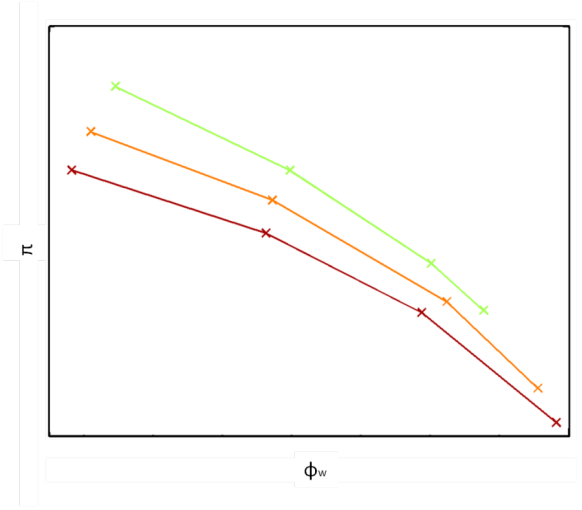

Figure 4.8: Illustration of the corrected pressure ratio for version 1. Brown line is dry gas. Orange and green line indicate two flows with different liquid mass fraction, where orange has a higher liquid mass fraction.

The calculated shaft power is increasing for increased liquid mass fractions. This can be seen in Figure 4.9.

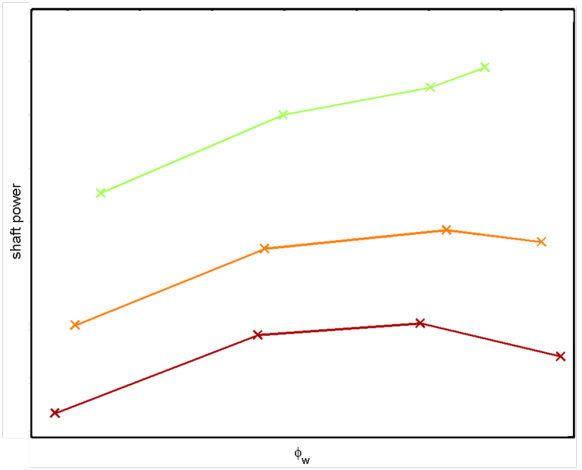

Figure 4.9: Illustration of the increase in power for version 1. Brown line is dry gas. Orange and green line indicate two flows with different liquid mass fraction, where orange has a higher liquid mass fraction.

Version 2

Version 2 differs from version 1 as it causes a higher enthalpy increase and thus a higher stage discharge temperature for the gas phase. The reduced range is received. By correcting the pressure coefficient and the polytropic efficiency, a steeper curve for increased liquid mass fraction is received. This can be seen in Figure 4.10.

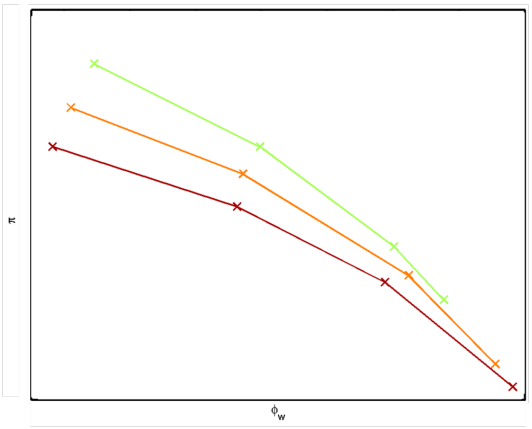

Figure 4.10: Illustration of the corrected pressure ratio for version 2. Brown line is dry gas. Orange and green line indicate two flows with different liquid mass fraction, where orange has a higher liquid mass fraction.

The result for the shaft power for version 2 is similar to the result for version 1. The increase in power due to increased liquid mass fraction in the flow is received. This can be seen in Figure 4.11.

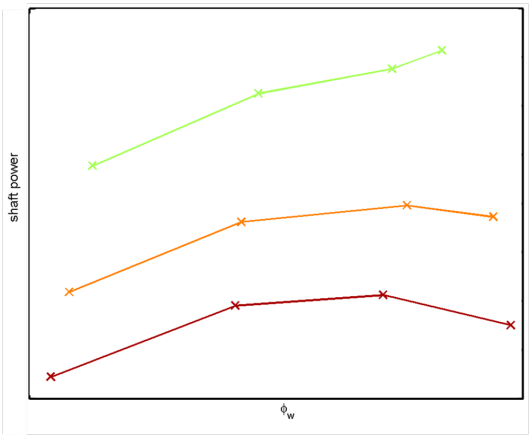

Figure 4.11: Illustration of the increase in power for version 2. Brown line is dry gas. Orange and green line indicate two flows with different liquid mass fraction, where orange has a higher liquid mass fraction.

5 Conclusions

This chapter summarizes the report. Results and findings are discussed. Thoughts about how to proceed are also presented.

5.1 Summary

In a wet gas compression process, all stream gas is compressed without pre-separation. The compression unit is smaller and lighter than a standard compression process.

Wet gas is defined as a gas with a liquid volume fraction of up to 5% within the oil and gas industry. The liquid phase introduces new physical processes to the gas. The new physical process gives additional challenges as thermal and phase equilibrium cannot be expected in all situations. The distribution of the liquid influences the impulse exchange between gas and liquid and thus pressure losses.

When compressing a wet gas, the required power increases and the maximum suction flow may be significantly reduced. Smaller maximum flow means a smaller operating range and steeper compressor curves. A higher pressure ratio compared to a dry reference run is seen for suction pressures around 1 bar, air/water mixture at liquid mass fractions below 10 %. For increased liquid mass fractions, the negative effects, such as increased friction losses dominate. For air/water mixtures at increased pressure levels, the interaction between the liquid and gas phase is more intense. For hydrocarbon mixtures at elevated suction pressure, a higher pressure ratio is received when increasing the liquid mass fractions. The effect on the pressure ratio is different depending on the composition of the wet gas mixture. When compressing a wet gas, the shaft power increases compared to a dry gas. One explanation to this is the increased density of the two-phase flow.

The dry gas model follows the measurements with an average relative error of less than 5 %. The errors can be explained by uncertainties in the measurement data and different implementations of the equation of state.

The wet gas model is based on the dry gas model. It is divided into a two-step correction. The first step contains a correction of the flow coefficient; the operating point is moved closer to choke. The first correction parameter is inspired by a homogenous model, which assumes that the velocities of the two phases are equal. It is depending on the gas volume fraction. The stage characteristics are thereafter corrected depending on which correction version used.

In version 1, the pressure coefficient is adjusted with a correction parameter inspired by a multiplier for two-phase flows in pipes. The computations for version 1 give an increase in pressure ratio and shaft power and a decrease in range.

The focus in version 2 is to adjust the power coefficient and the polytropic efficiency to be able to model the increase in shaft power, increased losses and increase in discharge pressure. The power increases about linearly with increased liquid mass fraction, the losses as well as the pressure changes with a function containing the rotational speed, density ratio and liquid mass fraction. The results for version 2 are similar to version 1, but steeper pressure ratio curves are received.

5.2 Outlook

The work performed in this Master Thesis is considered to be a first step. The models are based on models for multiphase flow in pipes.

When creating a model, it is important to use non-dimensional numbers to create a multiplier. The multipliers used in this report are non-dimensional and are based on the gas mass fraction, the gas volume fraction, the density ratio and a ratio of the impeller tip speed. These factors were observed to be the main factors for changes in the two-phase compression process, as described in Chapter 4.3 such that the effects of a wet gas were adequately resolved.

To move the compressor characteristics closer to choke for increased liquid mass fractions, by using the change in gas mass fraction is seen to be an effective method. To tune this correction parameter further to receive computations, which agree better with reality, would be of interest.

For version 1, the relations for multiphase flow in pipes were used with a correction for the rotational speed. The pressure coefficient was corrected to model the increase in discharge pressure, while keeping the discharge temperature about constant. This leads to increased polytropic efficiency, which is an indication on a more effective process. However, version 1 gives sufficient result for cases with increased discharge pressure. For cases where

there is no increased discharge pressure compared to the dry reference case, the correction parameter is too strong.

The correction using the gas volume fraction and the gas mass fraction shifts the characteristics closer to choke and decreases range, as seen in version 2. Compared to version 1, this version gives similar results but a steeper pressure ratio curve. To correct the power coefficient and the polytropic efficiency for the increase in power and higher losses, gives a higher discharge temperature. It would be of interest to investigate the change in discharge temperature for each phase, but as described, it is challenging to measure a single phase discharge temperature.

A further work of interest would be to extend version 1 and version 2 for the evaporation and condensation process through the compressor. Liquid droplets at the compressor discharge indicate that not all the liquid is evaporated. In literature, it has been seen that this would lead to a time-dependent and more complex model. To model the interaction between the liquid droplets and the gas flow more detailed, is a further implementation step. In this area the effects of the interaction between the liquid and the gas phase is proposed to be further investigated and also the impact of liquid droplets on the gas flow, concerning differences in phase velocities. The impact on the performance for different flow regimes in the compressor suction and through the compressor is suggested to be investigated. If the impact is high, these effects are suggested to be implemented in the model.

To be able to extend the model and make it more general, more experimental investigations and researches for different mixtures and compression conditions need to be analysed and evaluated. In the future, wet gas measurements from different types of machines and impellers are suggested to be evaluated and also different wet gas compositions at different suction pressure levels.

The effect of the stage design on the wet gas performance has not been investigated. The change in performance for a compressor for different types of impellers and stator designs is suggested to be mapped.

Acknowledgments

The last part of the five years of study in Mechanical Engineering at the Faculty of Engineering at Lund University has come to an end. The Master Thesis is performed at the Division of Thermal Power Engineering, Department of Energy Sciences.

The Master Thesis is carried out at MAN Diesel & Turbo Schweiz AG in Zürich, Switzerland during the summer of 2014. Two versions are written, one for the internal use within MAN and one for the Lund University, Faculty of Engineering, Division of Thermal Power Engineering at the Department of Energy Science in Sweden. The work load for this effort represents one semester, 30 ECTS.

The aim of the Master Thesis is to analyse the effects of compression of a wet gas and also to observe and analyse the effects on the thermal performance of a radial compressor when a liquid phase is present during the compression phase. A dry gas model is extended for a wet gas compression process. During the work, two main questions are handled:

- Is it possible to compress wet gas in a radial compressor?
- How is the compressor thermodynamic performance affected by a liquid phase in the compression process?

For approximately five years ago I started my studies at Lund University, Faculty of Engineering. At that time, I never thought that I would move to and live in Switzerland to write the Master Thesis five years later. During these five years, I specialized on power generation and I got the opportunity to move here.

The half year of Master Thesis writing has offered lots of ups and downs. I have learned a lot new about the area wet gas compression, but have also got further knowledge about Mat-Lab®. Thanks to both of my supervisors at MAN, Dr. Martin Scholtysik and Dr. Dirk Büche, for the support and discussions. It is a very interesting and challenging topic. I would also like to thank the Subsea team for the discussions in German. I have really improved it and enjoyed to work with you all.

I would also like to send a thank you to Sweden and the Associate Professor Magnus Genrup, who first made it possible for me to travel to and work in Switzerland in 2013 and have supported me during the Master Thesis work.

I would like to send a special thanks to Philipp Hecker, who has supported me during these six months.

Bibliography

[1] T. Knott. *"Subsea gas feels the pressure"*, Upstream Technology, vol. Q2, no. Q2, pp. 12-25, 2013.

[2] M. Chesshyre.*"Åsgard's case for subsea gas compression"*, Off-shore Engineer, no. December, pp. 50-51, 2010.

[3] L. Brenne, T. Bjoerge, J.L. Gilarranz, J.M. Koch, H. Miller,*"Performance evaluation of a centrifugal compressor operating under wet gas conditions"*. Texas, Houston: 34th Turbomachinery composium: 2005.

[4] L. Brenne, T. Bjoerge, L. E. Bakken, Øyvind Hundseid,*"Propspects for sub sea wet gas compression"*. Berlin, Germany, ASME Turbo Expo, GT2008-51158, 2008.

[5] H.I.H. Saravanamutto, GFC Rogers, H. Cohen, P.V. Straznicky. *"Gas Turbine Theory"*, Sixth edition. Harlow: Pearson Education Limited: 2009. ISBN 978-0-13-222437-6.

[6] K.H. Lüdtke. *"Process Centrifugal Compressors: Basics, function, operation, design, application"*. Berlin: Springer-Verlag Berlin Heidelberg GmbH: 2004. ISBN 978-3-642-07330-4.

[7] S.L. Dixon, C. A. Hall. *"Fluid Mechanics and Thermodynamics of Turbomachinery"*, Sixth edition. Burlington: Elsevier Inc: 2010. ISBN 978-1-85617-793-1.

[8] Y.A. Cengel, M.A. Boles. *"Thermodynamics: An engineering Approach"*, Fourth edition. New York: McGraw-Hill: 2002. ISBN 0-07-238332-1.

[9] J.D. Jr Anderson. *"Fundamentals of Aerodynamics"*, Fifth edition in SI units. New York: McGraw-Hills: 2011. ISBN 978-007-128908-5.

[10] B. Sundén, *"Värmeöverföring"*. Lund: Studentlitteratur: 2010. ISBN: 91-44-00087-1.

[11] Verein Deutsche Ingenieure, *"VDI Wärmeatlas - Recherchieren - Berechnen - Konstruieren"*, Ninth edition. Berlin: Springer-Verlag Berlin Heidelberg GmbH: 2002.

[12] P. von Böckh, *"Fluidmechanik Einführendes Lehrbuch"*, Second edition. Berlin: Springer-Verlag Berlin Heidelberg GmbH: 2002. ISBN: 3-540-22076-3.

[13] Endress-Hauser Flowtec AG, *"Durchfluss Handbuch"*, Fourth edition. Schaub Medien AG: 2003. ISBN: 3-9520220-3-9.

[14] G. Hetsroni, *"Chapter 3: Pressure Drop and Void Fraction"*, Short Courses - Modelling and Computation of Multiphase flows, vol. Part 1: Bases. pp: Chapter 3:1-36, 2006.

[15] D. Ransom, L. Podesta, M. Camatti, M. Wilcox, M. Bertoneri, M. Bigi, *"Mechanical Performance of a Two Stage Centrifugal Compressor under Wet Gas Conditions"*. Texas, Houston: 40th Turbomachinery Symposium, Houston, Texas, 2011.

[16] T.G. Grüner, L.E. Bakken, L. Brenne, T. Bjoerge, *"An experimental investigation of airfoil performance in wet gas flow"*. Berlin, Germany, ASME Turbo Expo, GT2008-50483, 2008.

[17] M. Bertoneri, S. Duni, D. Ransom, L. Podesta, M. Camatti, M. Bigi and M. Wilcox, *"Measured performance of two-stage centrifugal compressor under wet gas conditions"*. Denmark, Copenhagen, ASME Turbo Expo, GT2012-69819, 2012.

[18] Ö. Hundseid, L. Bakken, T. Grüner, L. Brenne and T. Bjoerge, *"Wet Gas Performance of a Single Stage Centrifugal Compressor"*. Germany, Berlin, ASME Turbo Expo, GT2008-51156, 2008.

[19] OpenModelica, *"Modelica Documentation"*. OpenModelica, [05 08 2014] [Online]. Available: https://build.openmodelica.org/Documentation/Modelica.Fluid.Dissipation.PressureLoss.StraightPipe.dp_ twoPhaseOverall_DP.html. [Accessed 04 08 2014].

[20] L.S. Tong, Y.S. Tang, *"Boiling Heat Transfer and Two-Phase Flow"*. Taylor and Francis Ltd. ISBN 1-56032-485-6.

[21] Shell Global Solutions International B.V., *"Gas/Liquid separators - Type selection and design rules"*. Shell, 2005.

[22] M. Fabbrizzi, C. Cerretelli, F. Del Medico and M. D'Orazio, *"An experimental investigation of a single stage wet gas centrifugal compressor"*. Orlando, Florida, USA, ASME Turbo Expo, GT2009-59548, 2009.

[23] M. Bertoneri, M. Wilcox, L. Toni and G. Beck, *"Development of Test Stand for Measuring Aerodynamic, Erosion and Rotordynamic Performance of a Centrifugal Compressor under Wet Gas Conditions"*. Düsseldorf, Germany, ASME Turbo Expo, GT2014-25349, 2014.

[24] M. Rennemo Jellum, *"Wet Gas Compressor Surge Detection"*. Norweigan University of Science and Technology, Trondheim, 2013.

[25] S. Madsen and L. E. Bakken, *"Gas Turbine Operation Off-Shore; Online Compressor Wash Operational Experience"*. Düsseldorf, Germany, ASME Turbo Expo, GT2014-25272, 2014.

[26] Ø. Hundseid, L. E. Bakken and T. Helde, *"A Revised Compressor Polytropic Performance Analysis"*. Barcelona, Spain, ASME Turbo Expo, GT2006-91033, 2006.

Appendix

Appendix 1

Thermodynamic Definitions

Thermal equilibrium	The phases in the system have equal temperatures. Definition used by VDI Wärmeatlas [11].
Mechanical equilibrium	The phases in the system have equal pressures. Definition used by Cengel and Boyles [8].
Thermodynamic equilibrium	The phases in the system have equal temperature and pressure. Definition used by VDI Wärmeatlas [11].
Phase equilibrium	There is no net mass transformation between the two-phases, which means that each phase in the system reaches a mass equilibrium. Definition used by Cengel and Boyles [8].
Surge line	Shows the lowest possible compressor suction flow with stable operating conditions. For operating conditions below this line flow instability and surge occur, which can cause damages to the turbomachine, according to Saravanamutto et al. [5].
Choke limit	Shows the upper limit on the suction flow for the turbomachine. The choke limit is the limit, where the compressor is not able to compress more inlet flow, according to definition used by Saravanamutto et al. [5].